

# Targeting *Plasmodium falciparum* IspD in the Methyl-*D*-Erythritol Phosphate Pathway: Urea-Based Compounds with Nanomolar Potency on target with low micromolar whole-cell activity

Daan Willocx,<sup>†,¶,‡</sup> Lorenzo Bizzarri,<sup>ψ,‡,¶</sup> Alaa Alhayek,<sup>ψ,†</sup> Patricia Bravo,<sup>§,||</sup> Boris Illarionov,<sup>⊥</sup> Katharina Rox,<sup>⊃,⊄</sup> Jonas Lohse,<sup>#</sup> Markus Fischer,<sup>⊥</sup> Andreas M. Kany,<sup>†</sup> Hannes Hahne,<sup>#</sup> Matthias Rottmann,<sup>§,||</sup> Matthias Witschel<sup>⊃</sup>, Mostafa M. Hamed,<sup>†</sup> Eleonora Diamanti,<sup>†</sup> Anna K. H. Hirsch<sup>\*,†,¶</sup>

<sup>†</sup>Helmholtz Institute for Pharmaceutical Research (HIPS), Helmholtz Centre for Infection Research (HZI), Saarland University, Campus E8.1, 66123 Saarbrücken, Germany

<sup>¶</sup>Saarland University, Department of Pharmacy, Campus E8.1, 66123 Saarbrücken, Germany

<sup>#</sup>OmicScouts GmbH, Lise-Meitner-Straße 30, 85354 Freising, Germany

<sup>§</sup>Swiss Tropical and Public Health Institute, Kreuzstrasse 2, 4123 Allschwil, Switzerland

<sup>⊃</sup>Helmholtz Centre for Infection Research (HZI), Department of Chemical Biology, Inhoffenstraße 7, 38124 Braunschweig, Germany

<sup>⊄</sup>German Center for Infection Research (DZIF), Partner site Hannover-Braunschweig, Inhoffenstraße 7, 38124 Braunschweig, Germany

<sup>||</sup>Universität Basel, Petersplatz 1, 4003 Basel, Switzerland

<sup>⊥</sup>Hamburg School of Food Science, University of Hamburg, Grindelallee 117, 20146 Hamburg, Germany

<sup>⊃</sup>BASF-SE, Carl-Bosch-Strasse 38, 67056 Ludwigshafen, Germany

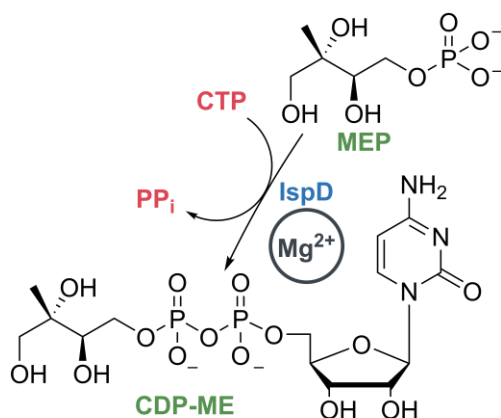
---

**ABSTRACT:** The methyl-*D*-erythritol phosphate (MEP) pathway has emerged as an interesting target in the fight against antimicrobial resistance. The pathway is essential in many human pathogens, including *Plasmodium falciparum* (*Pf*), but is absent in human cells, reducing the risk of off-target side effects. In the present study, we conducted a high-throughput screening on the third enzyme of the pathway, IspD, and discovered a new chemical class for which we ran a structure-activity relationship investigation, resulting in low-nanomolar inhibitors of *Pf*IspD. In addition, we determined the whole-cell activity (*Pf*NF54 IC<sub>50</sub> = 3.4 ± 1.0 μM), mode of inhibition, metabolic, and plasma stability of the new compound class. *In vivo* pharmacokinetic profiling of a selection of compounds demonstrated promising behavior for future development. Lastly, we disclosed a new MS-based enzymatic assay for direct IspD activity determination, circumventing the need for auxiliary enzymes. We used this assay to investigate the mode of inhibition of our new compound class. In summary, we have identified a readily synthesizable compound class, demonstrating excellent activity and a promising profile, positioning it as a valuable tool compound for advancing research on IspD.

---

Since the commercialization of penicillin in the 1940s, Sir Alexander Fleming warned the public about the dangers of antimicrobial resistance (AMR) resulting from over- and misuse of anti-infectives. Now, decades later, his warnings are more relevant than ever with AMR reaching alarming levels.<sup>1,2</sup> A recent example of newly developed resistance is the discovery of artemisinin-resistant strains of *Plasmodium falciparum* (*Pf*), one of the parasites that causes malaria, in Africa, Southeast Asia, the Pacific islands, and Latin America. Artemisinin-based treatments have been the ‘gold standard’ for malaria treatments for many years and resistance will have disastrous effects for malaria-prone regions.<sup>3</sup> The 2-*C*-methylerythritol-*D*-erythritol-4-phosphate (MEP) pathway, needed for the biosynthesis of the isoprenoid precursors isopentenyl diphosphate (IDP) and dimethylallyl diphosphate (DMADP), is an essential biosynthetic pathway in most Gram-negative bacteria, *Mycobacterium tuberculosis* and the *Plasmodium* parasites. Furthermore, the MEP pathway

is absent in human cells, mitigating the risk of off-target side effects, hence making it a source of promising drug targets.<sup>4,5</sup> Validation of the MEP pathway enzymes as drug target is based on fosmidomycin, an inhibitor of the second protein, IspC or DXR, of the MEP pathway. Currently in second-phase clinical trials as a combination treatment for malaria.<sup>6</sup> Within the present study, we focused on targeting the third enzyme in the MEP pathway, known as, IspD, MEP cytidyltransferase, or *ygbp*. IspD catalyzes the formation of 4-diphosphocytidyl-2-*C*-methylerythritol (CDP-ME) from MEP and cytidine triphosphate (CTP) in the presence of Mg<sup>2+</sup>, releasing inorganic diphosphate (PP<sub>i</sub>) (Scheme 1).<sup>7</sup> Previously reported inhibitors targeting *Pf*IspD can be subdivided into three chemical classes, namely, benzoisothiazolones **1**, identified by a combined approach of cheminformatics and high-throughput enzymatic screening, MMV008138 **2** recognized through phenotypic screening of the library of GlaxoSmithKline



**Scheme 1.** Reaction catalyzed by IspD starting from MEP and CTP affording CDP-ME.  $Mg^{2+}$  is the suspected cofactor in the reaction.

and lastly, a biphenyl carboxylic acid fragment **3** recently discovered by our group in collaboration with BASF (Figure 1). Despite the potential of IspD as a drug target, the number of IspD inhibitors reported is rather low, furthermore, the reported inhibitors are rather elaborated to synthesize or lack whole-cell activity.<sup>5, 8-12</sup> A possible cause might be the lack of a crystal structure of *PfIspD* available in the Protein Data Bank (PDB). Here, we report the structure-activity relationship (SAR) study of a new urea-based compound class targeting *PfIspD* with low nanomolar activity *in vitro*. Its synthesis is straightforward, in one step from the corresponding aniline and isocyanate. A high-throughput screening (HTS) approach on *Plasmodium vivax* IspD and subsequent confirmation of hits concomitantly on *PfIspD* and *PfNF54* led to the discovery of the initial hit (**4**, Figure 2) endowed with an  $IC_{50}$  of  $17 \pm 2 \mu M$  against *PfIspD* but lacking whole-cell activity. Synthesis of a total of 33 derivatives shed a light on the SAR of this newly discovered class reaching  $IC_{50}$  values as low as 41 nM and establishing whole-cell activity in low micromolar range. Throughout our study, we made efforts to maintain the easily synthesizable core of the urea class, ensuring the molecule's accessibility, given that antimalarials are predominantly utilized in low and middle-income countries.

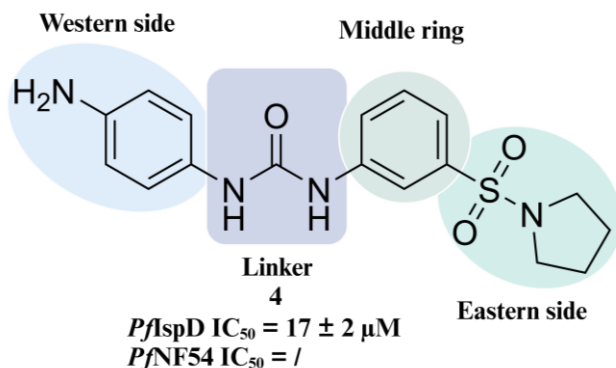
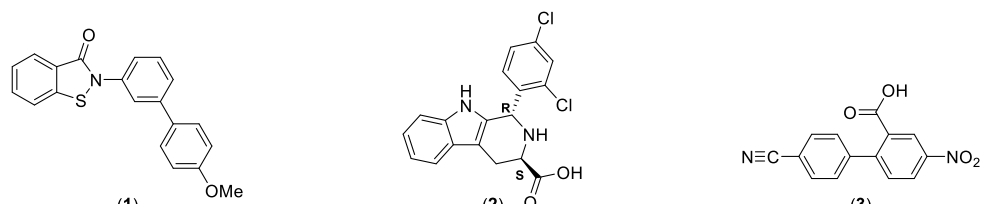


**Figure 2.** Initial hit compound (**4**) with an overview of the performed SAR study.

## RESULTS

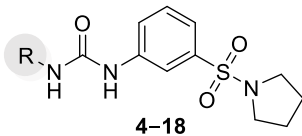
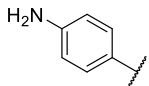
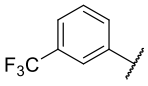
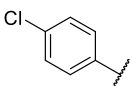
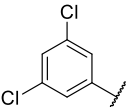
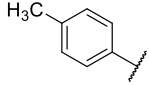
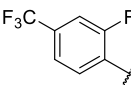
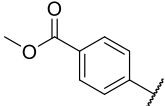
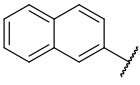
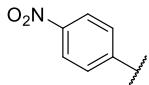
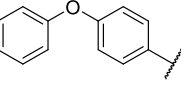
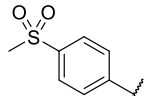
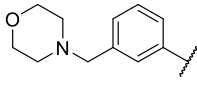
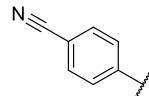
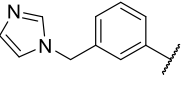
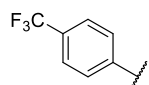
**SAR Exploration.** We commenced exploration of the initial hit by synthesizing derivatives with diverse moieties on the Western side phenyl ring (Figure 2). Compounds **4** – **18** were synthesized as depicted in Scheme 2. Depending on commercial availability, we either generated isocyanates *in situ* by reacting the respective amine with triphosgene or purchased them. Nucleophilic addition between 3-(pyrrolidin-1-ylsulfonyl)aniline and the respective isocyanate afforded the desired compounds. At first, we directed modifications towards the primary amine and replaced it by moieties with different electronic effects (**5–11**) (Table 1). We observed that more electron-withdrawing substituents, such as a nitro (**8**) or nitrile group (**10**), had a pronounced effect on the potency, resulting in a factor 400 increase (e.g., **8**,  $PfIspD IC_{50} = 41 \pm 7$  nM). While substituents with a less distinct electron-withdrawing effect, such as the trifluoromethyl (**11**) and the chloride (**5**), had a smaller effect on the potency (e.g., **11**,  $PfIspD IC_{50} = 91 \pm 19$  nM). Lastly, weak donating groups, such as the methyl (**6**), had an even smaller increase in potency (e.g., **6**,  $PfIspD IC_{50} = 370 \pm 80$  nM), but were still significantly better than the initial hit compound **4**. The reduced increase in potency of **9** ( $PfIspD IC_{50} = 330 \pm 40$  nM) could possibly be attributed to the size of the substituent as will be seen later. In addition, low micromolar activity in the whole-cell assay was noted for these derivatives. Next, we explored various substitution



Class	Benzoisothiazolones	MMV-08138	Biphenyl carboxylic acid
$PfIspD IC_{50} =$	210 nM	7.1 nM	151 $\mu M$
$EC_{50} =$	920 nM <sup>a</sup>	110 nM <sup>b</sup>	No data

**Figure 1.** Currently known classes of inhibitors showing enzymatic activity against *PfIspD*.  $EC_{50}$  values were measured against different strains of *Plasmodium falciparum*. <sup>a</sup>: strain = 3D7; <sup>b</sup>: strain = W2; Benzoisothiazolones <sup>8</sup> (**1**), MMV-08138<sup>9-12</sup> (**2**), Biphenylcarboxylic acid<sup>5</sup> (**3**).

**Table 1. *In vitro* and whole-cell activities for compounds 4–18**

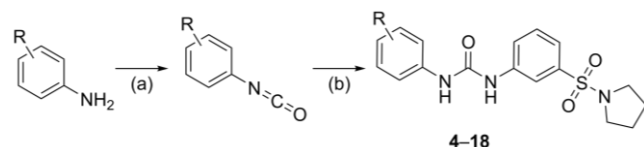
 4–18							
#	Structure, R=	<i>Pf</i> lspD (IC <sub>50</sub> nM) <sup>a</sup>	<i>Pf</i> NF54 (IC <sub>50</sub> μM) <sup>b</sup>	#	Structure, R=	<i>Pf</i> lspD (IC <sub>50</sub> nM) <sup>a</sup>	<i>Pf</i> NF54 (IC <sub>50</sub> μM) <sup>b</sup>
4		17000 ± 2000	n.a.	12		415 ± 60	5.0 ± 0.1
5		130 ± 12	38 ± 2	13		135 ± 30	7.4 ± 0.6
6		370 ± 80	37 ± 1	14		135 ± 30	8.7 ± 1.0
7		170 ± 20	n.a.	15		n.a.	23 ± 3
8		41 ± 7	8.5 ± 1.2	16		>1000	7.4 ± 1.0
9		330 ± 40	17 ± 1	17		>1000	6.5 ± 0.8
10		41 ± 11	10 ± 1	18		>1000	17 ± 3
11		91 ± 19	4.2 ± 0.5				

<sup>a</sup>Assays were performed in replicate as independent experiments ( $n \geq 2$ ); values are shown as mean ± SD. <sup>b</sup>Assays were performed in replicate as independent experiments ( $n = 2$ ); values are shown as mean ± SD. n.a. indicates the absence of activity.

patterns on the phenyl ring **12–14**. Placement of trifluoromethyl in *meta* position (**12**, *Pf*lspD IC<sub>50</sub> = 415 ± 60 nM) did not improve upon its *para*-substituted counterpart (**11**, *Pf*lspD IC<sub>50</sub> = 91 ± 19 nM). Furthermore, having multiple substituents (**13–14**) did also not lead to improvements in *Pf*lspD activity over the mono-substituted derivatives. To determine whether there was still room for growth on the Western side, we synthesized analogues **15–18** using the general synthetic route depicted in Scheme 2. Growth in this direction resulted in a significant loss in activity, which we interpret as a lack of

space for further expansions. For the remainder of the SAR, we decided to select **8** as scaffold and continued derivatization from its structure. Next, we focused on the urea linker itself (Table 2). Both positions of the urea bond were methylated successively as depicted in Scheme S1. To ensure selective methylation, **19** was synthesized by first transforming 3-(pyrrolidin-1-ylsulfonyl)aniline into the corresponding isocyanate with triphosgene, followed by addition of deprotonated *N*-methyl-4-nitroaniline to the reaction mixture. On the other hand, **20** was synthesized *via* two steps. First, a reductive amination between 3-

**Scheme 2. General synthetic procedure followed for the synthesis of 4–18<sup>a</sup>**



<sup>a</sup>Reagents and conditions: (a) triphosgene, Et<sub>3</sub>N, DCM, 0 °C to room temperature, 3 h, used as such in the next reaction step; (b) 3-(pyrrolidin-1-ylsulfonyl)aniline, DMF, room temperature, overnight, 8–95% yield.

(pyrrolidin-1-ylsulfonyl)aniline and paraformaldehyde resulted in *N*-methyl-3-(pyrrolidin-1-ylsulfonyl)aniline to which 1-isocyanato-4-nitrobenzene was added, resulting in a nucleophilic addition affording **20**. Unfortunately, methylation of either site of the urea bond led to complete loss of activity. A possible explanation for this observation could be the loss of hydrogen bonding interactions or conformational changes imposed by the methylation. Next we explored the possibility of replacing the urea with a thiourea (**21**) by employing an isothiocyanate in the synthesis instead of an isocyanate. This modification resulted as well in a decrease in activity (**21**, *PflspD* IC<sub>50</sub> = 395 ± 60 nM) in comparison with its urea counterpart (**8**, *PflspD* IC<sub>50</sub> = 41 ± 7 nM). Subsequent, modifications explored the Eastern side of the molecule (Figure 2). For the synthesis of these derivatives (**22–26**), we used the same synthetic procedure as depicted in scheme 2 with the only difference that the amine was varied instead of the isocyanate. Initially, we replaced the pyrrolidine with more flexible dimethyl (**22**) and diethyl (**23**) amine groups (Table 2). These derivatives did not manage to enhance activity (**22**, *PflspD* IC<sub>50</sub> = 180 ± 20 nM) over the pyrrolidine-containing parent compound (**8**, *PflspD* IC<sub>50</sub> = 41 ± 7 nM) (Table 2). Ring expansion towards piperidine and morpholine likewise failed to increase activity (**24–25**). On the other hand, when we substituted the pyrrolidine with a phenyl ring, the activity could be retained (**26**). Lastly, we explored a handful of compounds containing modifications on the middle ring (Table 3). Initially, these compounds were synthesized

**Table 2 *In vitro* and whole-cell activities for compounds 19–26.**

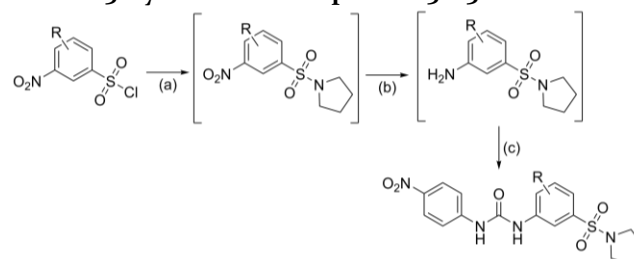
#	Structure, R=	<i>PflspD</i> (IC <sub>50</sub> nM) <sup>a</sup>	<i>PfNF54</i> (IC <sub>50</sub> μM) <sup>b</sup>
19		>1000	n.a.
20		>1000	8 ± 2.0
21		395 ± 60	15 ± 1.0

#	Structure, R=	<i>PflspD</i> (IC <sub>50</sub> nM) <sup>a</sup>	<i>PfNF54</i> (IC <sub>50</sub> μM) <sup>b</sup>
22		180 ± 20	n.a.
23		230 ± 25	3.4 ± 1.0
24		225 ± 20	16 ± 0.6
25		600 ± 110	8.1 ± 0.1
26		47 ± 7	9.6 ± 0.3

<sup>a</sup>Assays were performed in replicate as independent experiments ( $n \geq 2$ ); values are shown as mean ± SD. <sup>b</sup>Assays were performed in replicate as independent experiments ( $n = 2$ ); values are shown as mean ± SD. n.a. indicates the absence of activity.

containing a morpholine (**27–29**) instead of a pyrrolidine, as anilines of these derivatives were commercially available. Interestingly, compound **27** (*PflspD* IC<sub>50</sub> = 395 ± 3.5 nM) showed enhanced activity over parent compound **25** (*PflspD* IC<sub>50</sub> = 600 ± 110 nM). Consequently, we decided to construct derivatives containing the pyrrolidine (**30–36**). A three-step synthesis led to compounds **30–36** (Scheme 3). As a first step, a nucleophilic substitution reaction took place between pyrrolidine and the respective 3-nitrobenzenesulfonyl chloride. Next, the nitro group was reduced to the amine, which was then reacted with 1-isocyanato-4-nitrobenzene, affording the desired urea

**Scheme 3. Synthesis of compounds 30–36<sup>a</sup>**



<sup>a</sup>Reagents and reactions conditions: (a) respective 3-nitrobenzenesulfonyl chloride, pyrrolidine, triethylamine, acetonitrile, 0 °C, 5 min; (b) Fe powder, NH<sub>4</sub>Cl (166 mM in water), EtOH, 80 °C, 2.5 h; (c) 1-isocyanato-4-nitrobenzene, DMF, room temperature, 4 h, 5–37% yield over three steps.

**Table 3** *In vitro* and whole-cell activities for compounds 27–36

**25–34**

#	Structure, R <sup>1</sup> =	Structure, R <sup>2</sup> =	<i>Pf</i> IspD (IC <sub>50</sub> μM) <sup>a</sup>	<i>Pf</i> NF54 (IC <sub>50</sub> μM) <sup>b</sup>	#	Structure, R <sup>1</sup> =	Structure, R <sup>2</sup> =	<i>Pf</i> IspD (IC <sub>50</sub> μM) <sup>a</sup>	<i>Pf</i> NF54 (IC <sub>50</sub> μM) <sup>b</sup>
25			0.6 ± 0.1	8.1 ± 0.1	32			2.1 ± 0.3	16.9 ± 3.2
27			0.4 ± 0.1	7.3 ± 1.3	33			3.6 ± 0.4	11.0 ± 1.7
28			2.4 ± 0.3	2.7 ± 0.2	34			>10	15.3 ± 0.5
29			>10	6.9 ± 0.2	35			>10	9.7 ± 0.8
30			>10	6.3 ± 1.4	36			>10	18.0 ± 2.6
31			>10	18.4 ± 1.4					

<sup>a</sup>Assays were performed in replicate as independent experiments ( $n \geq 2$ ); values are shown as mean  $\pm$  SD. <sup>b</sup>Assays were performed in replicate as independent experiments ( $n \geq 2$ ); values are shown as mean  $\pm$  SD. n.a. indicates the absence of activity.

compounds (Table 3). After examination of these compounds in our *in vitro* assays, we could not observe any increase in potency over **8**, even not for the derivative containing the 4-fluoro moiety (**30**), which previously triggered a rise in potency. In summary, modifications directed at the Western side of the molecule are most influential towards the activity of the compound class. Positioning electron-withdrawing substituents at the *para* position induced the most notable changes, enabling compounds **8** and **10** to reach IC<sub>50</sub> values of 41 nM. Other substituents or further expansions at this position did not achieve such an increase in potency. In addition, an unsubstituted urea linker is detrimental for the activity of the compound class. Attempts to modify the middle ring turned out to be futile as any placement of a moiety led to a decrease in activity. On the Eastern side of the molecule, a pyrrolidine or phenyl ring led to the highest *in vitro* activity. Overall, compounds **8**, **10** and **26** are seen as frontrunners of the urea class, exhibiting the best *in vitro* activity, while also showing modest activity in the whole-cell assay. Interestingly, compound **26** constitutes a potential starting point to further explore the urea class by placing substituents on the phenyl ring or by growing in this direction.

**LC-MS based activity assay.** To gain an idea on the mode of inhibition of our new compound class, we intended to do a characterization of the enzyme kinetics under a range of inhibitor concentrations. Our intention was to perform this experiment without the influence of auxiliary enzymes inherent to the photometric assay used for IC<sub>50</sub> determinations.<sup>13</sup> To achieve this goal, we sought to uncover a way to measure the progress of the enzymatic reaction without relying on any secondary reactions. In our exploration, we encountered the work of Li *et al.*, who successfully profiled and quantified MEP metabolites in leaves using liquid chromatography–tandem mass spectrometry.<sup>14</sup> With this information in hand, we sought to develop an IspD activity assay based on the LC-MS detection and quantification of both substrate and product. Initial experiments revealed a significantly more pronounced signal for CDP-ME compared to MEP, with the latter often indistinguishable from background noise. An explanation for this observation might be the difference in ease of ionization, with CDP-ME being more readily ionizable than MEP. Furthermore, we observed identical fragmentation for MEP and the MEP part of CDP-ME,



resulting in an overestimation of the MEP concentration. Hence, we decided to continue the assay development relying on the quantification of the product, CDP-ME. Calibration curves measured for CDP-ME demonstrated a linear progression for a wide concentration range showing an  $R^2$  of 0.99 (Figure S1). Finally, an internal standard was chosen, initially several unreactive ATP derivatives, such as adenylyl-imidodiphosphate and adenosine-5'-[( $\alpha,\beta$ )-methylene]triphosphate were tested, but those exhibited long elution times of 20 to 30 minutes. Ultimately, we chose 4-methyl-1-oxo-1-(p-tolylamino)pentane-2-sulfonic acid as our internal standard, as its elution time was in the range of that of CDP-ME and showed consistent results.<sup>15</sup> To demonstrate the potential of our new assay, we determined the Michaelis constant ( $K_m$ ) of both substrates and obtained similar results as previously published (Table 4).<sup>10,12,16</sup> To our knowledge, this is the only reported IspD assay that is not dependent on auxiliary enzymes.

**Table 4. Comparison of Michaelis constants.**

	$K_m^{\text{CTP}}$ ( $\mu\text{M}$ )	$K_m^{\text{MEP}}$ ( $\mu\text{M}$ )
Our results <sup>a</sup>	58 $\pm$ 9	46 $\pm$ 3
Wu <i>et al.</i> <sup>12</sup>	Not reported	61
Imlay <i>et al.</i> <sup>10</sup>	59 $\pm$ 4	Not reported
Ghavami <i>et al.</i> <sup>16</sup>	9 $\pm$ 3	12 $\pm$ 3

<sup>a</sup>Assays were performed in replicate as independent experiments ( $n = 2$ ); values are shown as mean  $\pm$  SD

**Mode of inhibition.** Next, we measured the influence of **10** on the enzymatic kinetics of both substrates at different concentrations, ranging from 19.5 nM to 625 nM. The results, plotted in Lineweaver–Burk plots, hint towards a non-competitive inhibition of **10** towards CTP and uncompetitive towards MEP (Figure 3, Figure S2 and

**Table 5. *In vitro* metabolic and plasma stability of compounds 5, 8, 10 and 26**

Model system		5	8	10	26
Mouse Liver S9	$T_{1/2}$ [min] <sup>a</sup>	23 $\pm$ 3	11 $\pm$ 3	20 $\pm$ 5	23 $\pm$ 3
	$Cl_{\text{int}}$ [ $\mu\text{l}/\text{min}/\text{mg}$ ] <sup>a</sup>	31 $\pm$ 4	66 $\pm$ 20	36 $\pm$ 10	31 $\pm$ 4
Human Liver S9	$T_{1/2}$ (min) <sup>a</sup>	91 $\pm$ 19	53 $\pm$ 11	69 $\pm$ 12	>120
	$Cl_{\text{int}}$ [ $\mu\text{l}/\text{min}/\text{mg}$ ] <sup>a</sup>	8 $\pm$ 2	14 $\pm$ 3	10 $\pm$ 2	<5
Mouse Plasma	$T_{1/2}$ (min) <sup>a</sup>	>150	>150	>150	>150
	% at 2.5 h <sup>a</sup>	>100	>100	>100	>100
Human Plasma	$T_{1/2}$ [min] <sup>a</sup>	>150	>150	>150	>150
	% at 2.5 h <sup>a</sup>	>100	>100	>100	>100
HepG2 cytotoxicity	$CC_{50}$ [ $\mu\text{M}$ ] <sup>a</sup>	29 $\pm$ 7	62 $\pm$ 15	40 $\pm$ 5	>100

<sup>a</sup>Assays were performed in duplicate as independent experiments ( $n = 2$ ); values are shown as mean  $\pm$  SD

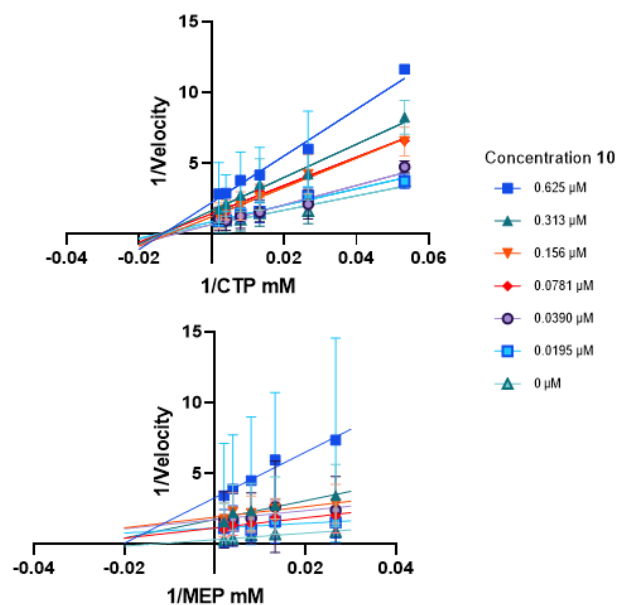


**Figure 3.** The inhibition of *PflspD* by **10** is characterized as non-competitive with CTP, while uncompetitive with MEP. Lineweaver-Burk plots of both substrates at varying concentrations of **10**. Above: CTP was varied; below: MEP concentration was varied.

Figure S3). This finding indicates that compound **10** binds to *PflspD* in a manner independent of CTP binding to the active site. In this way, it influences the catalytic activity of the enzyme without affecting CTP binding. This highlights an allosteric inhibition mechanism of the enzyme, which, has been observed before for *Arabidopsis thaliana* IspD by Witschel and coworkers but has never been observed previously for *PflspD*.<sup>17</sup> On the other hand, compound **10** selectively targets the *PflspD*-MEP complex, influencing the catalytic activity of the enzyme as well as the substrate binding.

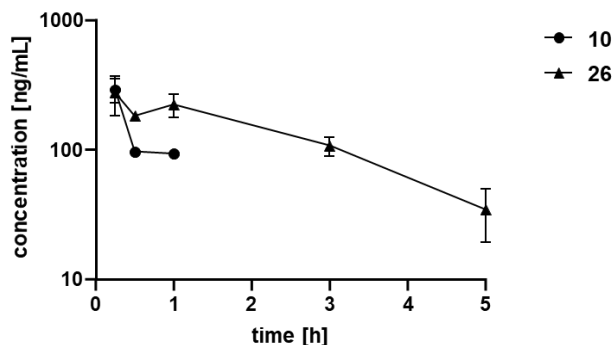


**Figure 5.** PK plasma profile over time of **10** and **26** at 1 mg/kg IV.

These findings elucidate the selectivity of compound **10** against both substrates, revealing distinct modulatory effects dependent on the substrate specificity of *PflspD*.

**Metabolic and Plasma Stability.** To gain an initial understanding of selected ADMET properties of the urea class, the metabolic and plasma stability of selected compounds (**5**, **8**, **10**, **26** and **37**), was determined in liver S9 fractions and plasma of both mouse and human (Table 5). Clearance in mouse S9 liver fraction was high to moderate, with compounds **5**, **6** and **26** showing lower clearance than **8** and **37**. In human S9, clearance showed a similar trend with generally lower turnover. No metabolism during 120 min was observed in human S9 fractions for **26**. Regarding plasma stability, all selected compounds showed complete stability in both species (Table 5). Lastly, we also assessed the cytotoxicity towards HepG2 cells. No significant cytotoxicity was observed for **26** up to 100  $\mu$ M, while the other compounds showed an  $IC_{50}$  range of 29 – 62  $\mu$ M.

**Pharmacokinetic (PK) profiling.** As several compounds exhibited promising initial ADMET properties, we embarked on *in vivo* PK studies with compounds **10** and **26**. We administered both compounds in a cassette format *via* the intravenous (IV) route at

<i>In vivo</i> PK <sup>a</sup>	<b>10</b>	<b>26</b>
$T_{1/2}$ [h]	0.05 $\pm$ 0.1	1.55 $\pm$ 0.5
$C_0$ [ng/mL]	912.6 $\pm$ 400.2	433.1 $\pm$ 256.6
$AUC_{0-t}$ [ng/mL*h]	246.4 $\pm$ 63.3	717.4 $\pm$ 135.9
MRT [h]	0.6 $\pm$ 0.2	2.24 $\pm$ 0.7
$V_{z\_obs}$ [L/kg]	2.5 $\pm$ 0.8	2.9 $\pm$ 1.2
$Cl_{obs}$ [mL/min/kg]	53.0 $\pm$ 8.5	20.9 $\pm$ 2.0
Liver ng/g	ND	202.6 $\pm$ 45.8

<sup>a</sup>Assays were performed in replicate as independent experiments ( $n = 2$  animals); values are shown as mean  $\pm$  SD.  $AUC_{0-t}$  = area under the concentration-time curve from time zero to time  $t$ ; MRT = mean residence time;  $V_{z\_obs}$  = observed volume of distribution;  $Cl_{obs}$  = observed clearance (based on

observed last time point with measurable concentration); ND = not detected

1 mg/kg. Whereas compound **10** exhibited a short half-life of only 0.5 h, **26** had a half-life of around 1.6 h suggesting additional clearance mechanisms *in vivo* for compound **10** compared to **26** as the latter had a lower observed plasma clearance compared to **10**. Furthermore, both compounds had a similar volume of distribution of around 2.5–2.9 L/kg, suggesting that compounds might also distribute into tissue (Table 6). Moreover, **26** was still detectable until 5 hours and had higher exposure levels (Figure 5). When looking at terminal organ concentrations, **26** was found at around 203 ng/g tissue in liver, whereas **10** was not detected. This demonstrated that **26** had already favorable PK properties for further development.

## DISCUSSION

With our SAR, we accomplished a 400-fold increase in inhibitory activity of IspD, while also achieving activity in a whole-cell assay (Figure 6). Modifications directed to the Western side of the molecule were most impactful towards the increase in potency, and achieving whole-cell activity. Furthermore, trying to grow at this side of the molecule indicated that there is no space in the binding pocket to further expand in this direction. Adjustments directed at the urea linker, taught us that an unsubstituted urea bond is key for the activity. From there on, modifications directed to the middle ring and Eastern side of the scaffold did not result in further enhancement of the potency. Development of the new LC-MS based activity assay allowed us to gain an idea of the mode of inhibition of this new compound class without the use of auxiliary enzymes. Ultimately, this led to the confirmation of non-competitive inhibition of **10** towards CTP and uncompetitive towards MEP. Therefore, the whole SAR could potentially teach us something about the structure of the allosteric pocket of *PflspD*. Structural information of the allosteric pocket could facilitate future research towards *PflspD* inhibitors. Especially as the active site of IspD appears to be challenging to target due to its very polar character and solvent-exposure. Lastly, the metabolic clearance and plasma stability experiments demonstrated moderate to good values for some of the representative compounds of the urea class, which were confirmed by *in vivo* PK studies, revealing compound **26** with the best PK properties.

## CONCLUSIONS

In summary, through a HTS campaign, we discovered a new hit compound with an  $IC_{50}$  value in the low micromolar range against *PflspD*. Conducting SAR around this new chemical entity led to a 400-fold increase in *in vitro* potency and achieved whole-cell activity (Figure 6). The *in vitro* activity of the urea class is on par with other *PflspD* inhibitors, with the added benefit of a straightforward synthesis. Utilizing our newly developed LC-MS based IspD assay, we gained insights on the mode of inhibition of our new chemical class, which points towards an allosteric inhibition mechanism. Lastly, initial ADMET and PK studies confirmed the potential of the new

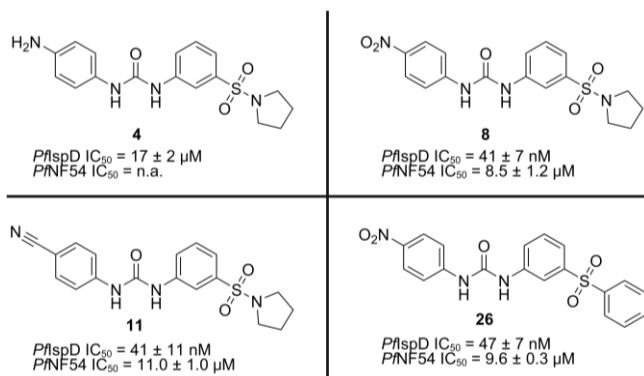


**Figure 6.** Initial hit compound and the best performing urea class derivatives. n.a. no activity.

class for further development. Overall, due to its potent inhibitory activity, ease to synthesize, interesting mode of inhibition, and good ADMET profile, the urea class has a great potential for further development in the anti-infective field.

### EXPERIMENTAL SECTION

**General.** Purity of all compounds used in biochemical assays was ≥ 95%. Be aware, in contact with water, triphosgene is converted to the extremely toxic phosgene gas. Starting materials and solvents were purchased from commercial suppliers, and used without further purification. All chemical yields refer to purified compounds and were not optimized. Column chromatography was performed using the automated flash chromatography system CombiFlash®Rf (Teledyne Isco) equipped with RediSepRf silica columns. Preparative RP-HPLC was performed either using an UltiMate 3000 Semi-Preparative System (Thermo Fisher Scientific) equipped with nucleodur®C18 Gravity (250 mm × 16 mm, 5 μm) column or using a Pure C-850 Flash/Prep (Buchi) equipped with Nucleodur C18 HTec (250 mm × 40 mm, particle size 5 μm). Low resolution mass spectrometry and purity control of final compounds was carried out using an Ultimate 3000-MSQ LCMS system (Thermo Fisher Scientific) consisting of a pump, an autosampler, MWD detector and an ESI quadrupole mass spectrometer. <sup>1</sup>H and <sup>13</sup>C NMR spectra were recorded as indicated on a Bruker Avance Neo 500 MHz (<sup>1</sup>H, 500 MHz; <sup>13</sup>C, 126 MHz) with prodigy cryoprobe system. Chemical shifts were recorded as δ values in ppm units and referenced against the residual solvent peak (DMSO-*d*<sub>6</sub>, δ= 2.50, 39.52 and acetone-*d*<sub>6</sub>: δ=2.05, 29.84, CD<sub>3</sub>OD: δ= 3.27, 47.6). Splitting patterns describe apparent multiplicities and are designated as s (singlet), br s (broad singlet), d (doublet), dd (doublet of doublet), t (triplet), q (quartet), m (multiplet). Coupling constants (J) are given in Hertz (Hz). High-resolution mass spectra were recorded on a ThermoFisher Scientific (TF, Dreieich, Germany) Q Exactive Focus system equipped with heated electrospray ionization (HESI)-II source. For the LC-MS based IspD assay, a TF UltiMate 3000 binary RSLC UHPLC (Thermo Fisher, Dreieich, Germany)

equipped with a degasser, a binary pump, an autosampler, and a thermostated column compartment and a MWD, coupled to a TF TSQ Quantum Access Max mass spectrometer with heated electrospray ionization source (HESI-II) was used. The separation was performed with a SeQuant ZIC-HILIC 5 μm polymeric HPLC column (100 × 2.1 mm) with a precolumn at flow rate of 0.225 μL/min with a mobile phase composed of 50 mM ammonium acetate pH 8.5 (elute A), ACN (eluent B) under the following conditions: 0 – 30 sec 80% B, 30 – 105 sec 70% B, 105 – 135 sec 70–40% B, 135 – 300 sec hold, and 300 – 420 sec 80% B with 225 μL/min flow rate and a total run time of 7 min. The divert valve was set to 0.49 min. The injection volume was 5 μL. The temperature of the autosampler was set to 6 °C. The following MS settings were used: electrospray ionization (ESI); negative mode for CDP-ME and MEP; collision gas pressure: 1.5 Torr; spray voltage: 10 V. The mass spectrometer was operated in the SRM mode with the following masses: 520.116 (fragment: 322.135 - 322.145) m/z for CDP-ME (tube lens offset 93 V and collision energy 23 eV); 215.006 (fragment: 79.395 - 79.405, 97.395 - 97.405) m/z for MEP (tube lens offset 94 V and collision energy 23 and 47 eV, respectively); 284.07 (fragment: 106.19, 177.03 - 150.15) m/z for 4-methyl-1-oxo-1-(p-tolylamino)pentane-2-sulfonic acid (tube lens offset 28 and 21 respectively V and collision energy 28 and 21 eV, respectively) with a scan width of 0.010 m/z and a scan time of 0.1 s, respectively. Observed retention times were as follows: CDP-ME, MEP, and 4-methyl-1-oxo-1-(p-tolylamino)pentane-2-sulfonic acid 4.90, 4.72, and 1.04 min, respectively (Figure S4). MS-peak areas were determined using TF Xcalibur Software then CDP-ME and MEP peak areas were normalized by the internal standard peak area. All PK plasma samples were analyzed via HPLC-MS/MS using an Agilent 1290 Infinity II HPLC system coupled to an AB Sciex QTrap 6500plus mass spectrometer. HPLC conditions were as follows: column: Agilent Zorbax Eclipse Plus C18, 50x2.1 mm, 1.8 μm; temperature: 30 °C; injection volume: 5 μL; flow rate: 700 μL/min; solvent A: water + 0.1% formic acid; solvent B: acetonitrile + 0.1% formic acid; gradient for 10 and 26: 99% A at 0 min, 99% - 0% A from 0.1 min to 4.0 min, 0 % A until 4.5 min. Mass spectrometric conditions were as follows: Scan type: Q1 and Q3 masses for glipizide, 10 and 26 can be found in Table S1; peak areas of each sample and of the corresponding internal standard were analyzed using Multi-Quant 3.0 software (AB Sciex).

### Chemistry.

**General procedure 1 (GP-1) for the synthesis of analogues 5–12.** To a flask containing 3-(pyrrolidin-1-ylsulfonyl)aniline (1 equiv), and DMF (150 equiv, unless otherwise stated), the respective isocyanate (1 equiv) was added at 0 °C. The resulting mixture was stirred at room temperature overnight, after which, water was added, and the resulting mixture was extracted with EtOAc (3x, 20mL). The combined organic layers were washed with



saturated aqueous NaCl solution, dried over MgSO<sub>4</sub>, filtered, concentrated *in vacuo*, and purified.

**General procedure 2 (GP-2) for the synthesis of analogues 13–18.** To a flask that contains triphosgene (0.5 equiv) in DCM (150 equiv, unless otherwise stated) at 0 °C under argon atmosphere, a solution of DCM (150 equiv, unless otherwise stated) containing the respective amine (1.2 equiv) and trimethylamine (1.2 equiv) was added and resulting mixture was stirred at room temperature for 3 h. Next, a flask was charged with 3-(pyrrolidin-1-ylsulfonyl)aniline (1 equiv), NaH 60% (1.2 equiv) and DMF (150 equiv), the resulting mixture was stirred for 1 h under argon atmosphere, after which, the solution was added dropwise to the flask containing the triphosgene reaction mixture and the resulting solution was stirred at room temperature overnight. Water (20 mL) was added and the mixture was extracted with EtOAc (3x, 20mL), washed with saturated aqueous NaCl solution, dried over MgSO<sub>4</sub>, filtered, concentrated *in vacuo*, and purified.

**General procedure 3 (GP-3) for the synthesis of analogues 22–29.** To a flask containing 1-isocyanato-4-nitrobenzene and DMF (150 equiv, unless otherwise stated), the respective aniline (1 equiv) was added at room temperature. The resulting mixture was stirred at room temperature overnight, after which, water was added and the resulting mixture was extracted with EtOAc (3x, 20mL). The combined organic layers were washed with saturated aqueous NaCl solution, dried over MgSO<sub>4</sub>, filtered, concentrated *in vacuo*, and purified.

**General procedure 4 (GP-4) for the synthesis of analogues 30–34.** To a flask containing acetonitrile (100 equiv), trimethylamine (2 equiv), and pyrrolidine (1 equiv) at 0 °C, the respective 3-nitrobenzenesulfonyl chloride (1 equiv) was added. Next the resulting solution was stirred for 5 min at 0 °C, after which, the solvent was evaporated. To the residue, EtOH (140 equiv), an aqueous solution of NH<sub>4</sub>Cl at a concentration of 166 mM (0.50 equiv), and Fe powder (5 equiv) were added, the resulting reaction mixture was stirred at 80 °C for 2.5 h. Next, the organic solvent was evaporated *in vacuo*, water (20 mL) was added, and the solution was extracted with EtOAc (3x, 20mL). The combined organic layers were dried over MgSO<sub>4</sub>, filtered, and concentrated *in vacuo*. Subsequent, the residue was solubilised with DMF (45 equiv), and 1-isocyanato-4-nitrobenzene (1.5 equiv) was added. The resulting reaction mixture was stirred at room temperature for 1 h, after which, DMF was removed on reduced pressure and the residue was purified.

**1-(4-Aminophenyl)-3-(3-(pyrrolidin-1-ylsulfonyl)phenyl)urea (4)** A mixture of 1-(4-nitrophenyl)-3-(3-(pyrrolidin-1-ylsulfonyl)phenyl)urea (**8**) (0.15 g, 0.4 mmol), Fe (0.11 mg, 1.9 mmol), and ammonium chloride (0.01 g, 0.2 mmol) was dissolved in an ethanol/water (2:1) mixture. The mixture was heated to 100 °C for 2 hours. Excess ethanol was evaporated *in vacuo*, and the remaining residue was washed with water (3x, 20 mL), and then filtered. The obtained solid was then purified using preparative HPLC affording **4** as a white powder (0.1 g, 72% yield).

<sup>1</sup>H NMR (500 MHz, DMSO-*d*<sub>6</sub>) δ 10.60 (s, 1H), 10.51 (s, 1H), 8.22 (d, *J* = 9.1, 2H), 8.08 (s, 1H), 7.82 (d, *J* = 9.1, 2H), 7.75 (d, *J* = 7.9, 1H), 7.61 (t, *J* = 7.8, 1H), 7.56 (d, *J* = 7.8, 1H), 3.17 (t, *J* = 6.6, 4H), 1.66 (t, *J* = 6.6, 4H). <sup>13</sup>C NMR (126 MHz, DMSO-*d*<sub>6</sub>) δ 179.7, 145.8, 142.6, 140, 136.2, 129.7, 127.5, 124.5, 123.3, 122.2, 121.8, 47.9, 24.8. HR-MS (ESI) calculated for C<sub>17</sub>H<sub>21</sub>N<sub>4</sub>O<sub>3</sub>S [M + H]<sup>+</sup>: 361.1256, found: 361.1327

**1-(4-Chlorophenyl)-3-(3-(pyrrolidin-1-ylsulfonyl)phenyl)urea (5).** According to GP-1, using 1-chloro-4-isocyanatobenzene (0.08 g, 0.49 mmol), affording after purification by flash chromatography (CH<sub>2</sub>Cl<sub>2</sub>/MeOH, 10/0 → 9.5/0.5), and washing with MeOH, **5** was afforded as a white powder (22 mg, 11% yield). <sup>1</sup>H NMR (500 MHz, DMSO-*d*<sub>6</sub>) δ 9.1 (s, 2H), 8.1 (t, *J* = 2.0, 1H), 7.7–7.6 (m, 1H), 7.6–7.5 (m, 3H), 7.4 (d, *J* = 7.7, 1H), 7.4–7.3 (m, 2H), 3.2–3.1 (m, 4H), 1.7–1.6 (m, 4H). <sup>13</sup>C NMR (126 MHz, DMSO-*d*<sub>6</sub>) δ 152.9, 141, 138.9, 137, 130.3, 129.1, 126.1, 122.7, 120.8, 120.5, 116.9, 48.3, 25.2. HR-MS (ESI) calculated for C<sub>17</sub>H<sub>19</sub>ClN<sub>3</sub>O<sub>3</sub>S [M+H]<sup>+</sup>, 380.0757, found: 380.0822. HPLC purity: 98%.

**1-(3-(Pyrrolidin-1-ylsulfonyl)phenyl)-3-(*p*-tolyl)urea (6).** According to GP-1, using *p*-tolyl isocyanate (0.06 mL, 0.48 mmol), affording after purification by flash chromatography (cyclohexane/EtOAc = 1:1) **6** as white solid (0.15 g, 95% yield). <sup>1</sup>H NMR (500 MHz, DMSO-*d*<sub>6</sub>) δ 9.0 (s, 1H), 8.7 (s, 1H), 8.1 (t, *J* = 2.0, 1H), 7.6–7.5 (m, 1H), 7.5 (t, *J* = 7.9, 1H), 7.4–7.3 (m, 3H), 7.1 (d, *J* = 8.3, 2H), 3.2–3.1 (m, 4H), 2.3 (s, 3H), 1.7–1.6 (m, 4H). <sup>13</sup>C NMR (126 MHz, DMSO-*d*<sub>6</sub>) δ 153, 137.2, 137, 131.5, 130.2, 129.7, 122.5, 120.6, 119.1, 116.7, 48.3, 25.2, 20.8. HR-MS (ESI) calculated for C<sub>18</sub>H<sub>22</sub>N<sub>3</sub>O<sub>3</sub>S [M + H]<sup>+</sup>, 360.1304, found: 360.1361. HPLC purity: 99%.

**Methyl 4-(3-(3-(pyrrolidin-1-ylsulfonyl)phenyl)ureido)benzoate (7).** According to GP-1, using methyl 4-isocyanatobenzoate (0.088 g, 0.5 mmol), and CH<sub>2</sub>Cl<sub>2</sub> (10 mL), to afford after filtration of the precipitate, **7** as a white solid (0.15 g, 75% yield). <sup>1</sup>H NMR (500 MHz, DMSO-*d*<sub>6</sub>) δ 9.2 (br s, 2H), 8.1 (t, *J* = 1.8 Hz, 1H), 7.9 (d, *J* = 8.7 Hz, 2H), 7.7–7.6 (m, 3H), 7.6 (t, *J* = 7.9 Hz, 1H), 7.4 (d, *J* = 7.6 Hz, 1H), 3.8 (s, 3H), 3.2–3.1 (m, 4H), 1.7–1.6 (m, 4H). <sup>13</sup>C NMR (126 MHz, DMSO-*d*<sub>6</sub>) δ 166.4, 152.7, 144.5, 140.7, 137.1, 130.9, 130.4, 123.2, 122.8, 121.1, 118.1, 117.1, 52.3, 48.3, 25.2. HR-MS (ESI) calculated for C<sub>19</sub>H<sub>22</sub>N<sub>3</sub>O<sub>5</sub>S [M + H]<sup>+</sup>: 404.1202, found: 404.1275. HPLC purity: 98%.

**1-(4-Nitrophenyl)-3-(3-(pyrrolidin-1-ylsulfonyl)phenyl)urea (8).** According to GP-1, using 1-isocyanato-4-nitrobenzene (0.1 g, 0.61 mmol), to afford after purification by flash chromatography (CH<sub>2</sub>Cl<sub>2</sub>/MeOH, 10/0 → 9.5/0.5), **8** as a yellow powder (0.02 g, 8% yield). <sup>1</sup>H NMR (500 MHz, DMSO-*d*<sub>6</sub>) δ 9.6 (br s, 1H), 9.4 (br s, 1H), 8.2 (br d, *J* = 8.9 Hz, 2H), 8.1 (br s, 1H), 7.7 (br d, *J* = 8.4 Hz, 2H), 7.7 (br d, *J* = 7.6 Hz, 1H), 7.6 (br t, *J* = 7.9 Hz, 1H), 7.4 (br d, *J* = 7.6 Hz, 1H), 3.2–3.1 (m, 4H), 1.7 (br s, 4H). <sup>13</sup>C NMR (126 MHz, DMSO-*d*<sub>6</sub>) δ 152.1, 146.1, 141.2, 140, 136.6, 129.9, 125.1, 122.5, 120.9, 117.9, 117.8, 116.8, 47.9, 24.7. HR-MS (ESI) calculated for C<sub>17</sub>H<sub>19</sub>N<sub>4</sub>O<sub>5</sub>S [M + H]<sup>+</sup>: 391.0998, found: 391.1066. HPLC purity: 100%.

**1-(4-(Methylsulfonyl)phenyl)-3-(3-(pyrrolidin-1-ylsulfonyl)phenyl)urea (9).** According to GP-1, using 1-isocyanato-4-(methylsulfonyl)benzene (0.99 g, 0.5 mmol) and, DCM (10 mL), to afford after filtration of the

precipitate **9** as a white powder (0.15 g, 70% yield). <sup>1</sup>H NMR (500 MHz, DMSO-*d*<sub>6</sub>) δ 9.29 (br s, 2H), 8.1–8.0 (m, 1H), 7.8 (d, *J* = 8.9 Hz, 2H), 7.7 (d, *J* = 8.9 Hz, 2H), 7.7–7.6 (m, 1H), 7.5 (t, *J* = 7.9 Hz, 1H), 7.4 (d, *J* = 7.8 Hz, 1H), 3.2–3.1 (m, 7H), 1.7–1.6 (m, 4H). <sup>13</sup>C NMR (126 MHz, DMSO-*d*<sub>6</sub>) δ 152.7, 144.7, 140.6, 137.1, 133.9, 130.4, 128.8, 122.9, 121.2, 118.5, 117.2, 48.3, 44.4, 25.2. HR-MS (ESI) calculated for C<sub>18</sub>H<sub>22</sub>N<sub>3</sub>O<sub>5</sub>S<sub>2</sub> [M + H]<sup>+</sup>: 424.0923, found: 424.0997. HPLC purity: 99%.

*1-(4-Cyanophenyl)-3-(3-(pyrrolidin-1-ylsulfonyl)phenyl)urea (10)*. According to **GP-1**, using 4-isocyanatobenzonitrile (0.1 g, 0.69 mmol), to afford after purification by flash chromatography (CH<sub>2</sub>Cl<sub>2</sub>/MeOH, 10/0 → 9.5/0.5) and recrystallization with CH<sub>2</sub>Cl<sub>2</sub>, and diethyl ether, **10** as a yellow powder (0.075 g, 29 % yield). <sup>1</sup>H NMR (500 MHz, DMSO-*d*<sub>6</sub>) δ 9.3 (br s, 2H), 8.1 (t, *J* = 1.8 Hz, 1H), 7.8–7.7 (m, 2H), 7.7–7.6 (m, 2H), 7.7–7.6 (m, 1H), 7.6 (t, *J* = 7.9 Hz, 1H), 7.4 (d, *J* = 7.8 Hz, 1H), 3.2–3.1 (m, 4H), 1.7–1.64 (m, 4H). <sup>13</sup>C NMR (126 MHz, DMSO-*d*<sub>6</sub>) δ 152.6, 144.4, 140.6, 137.1, 133.8, 130.4, 123, 121.3, 119.7, 118.8, 117.2, 104.1, 49.1, 48.3, 25.2. HR-MS (ESI) calculated for C<sub>18</sub>H<sub>19</sub>N<sub>4</sub>O<sub>3</sub>S [M + H]<sup>+</sup>: 371.1010, found: 371.1157. HPLC purity: 98%.

*1-(3-(Pyrrolidin-1-ylsulfonyl)phenyl)-3-(4-(trifluoromethyl)phenyl)urea (11)*. According to **GP-1**, using 1-isocyanato-4-(trifluoromethyl)benzene (0.09 g, 0.5 mmol), and DCM (10 mL), to afford after filtration of the precipitate, **11** as an off-white powder (0.09 g, 0.213 mmol, 43% yield). <sup>1</sup>H NMR (500 MHz, DMSO-*d*<sub>6</sub>) δ 9.2 (s, 1H), 8.1 (t, *J* = 1.8 Hz, 1H), 7.7–7.6 (m, 1H), 7.6–7.5 (m, 1H), 7.5 (t, *J* = 7.9 Hz, 1H), 7.4 (d, *J* = 7.8 Hz, 1H), 3.2–3.1 (m, 1H), 1.7–1.6 (m, 1H). <sup>13</sup>C NMR (126 MHz, DMSO-*d*<sub>6</sub>) δ 152.8, 143.6, 140.7, 137.1, 130.4, 126.7–126.5 (m), 122.9, 121.1, 118.7, 117.1, 48.3, 25.2. <sup>19</sup>F NMR (470 MHz DMSO-*d*<sub>6</sub>) δ -60.1. HR-MS (ESI) calculated for C<sub>18</sub>H<sub>9</sub>F<sub>3</sub>N<sub>3</sub>O<sub>3</sub>S [M + H]<sup>+</sup>: 414.1021, found: 414.1087. HPLC purity: 99%.

*1-(3-(Pyrrolidin-1-ylsulfonyl)phenyl)-3-(3-(trifluoromethyl)phenyl)urea (12)*. According to **GP-1**, using 1-isocyanato-3-(trifluoromethyl)benzene (0.07 g, 0.35 mmol), to afford after purification by flash chromatography (EtOAc/petroleum ether, 3/7 → 5/5), recrystallization using MeOH, and washing with CH<sub>2</sub>Cl<sub>2</sub> (3x, 5 mL), **12** as a white crystalline powder (0.01 g, 8% yield). <sup>1</sup>H NMR (500 MHz, CD<sub>3</sub>OD) δ 8.1 (t, *J* = 1.9 Hz, 1H), 7.9 (s, 1H), 7.7 (ddd, *J* = 8.0, 2.2, 1.2 Hz, 1H), 7.6 (dd, *J* = 8.2, 1.6 Hz, 1H), 7.6–7.5 (m, 1H), 7.5–7.4 (m, 2H), 7.3–7.2 (m, 1H), 3.3–3.2 (m, 4H), 1.8–1.7 (m, 4H). <sup>13</sup>C NMR (126 MHz, CD<sub>3</sub>OD) δ 153.3, 140.2, 140, 137.2, 129.4 (d, *J* = 4.4), 125.3, 123.1, 122.7, 122, 121.1, 118.8, 117.4, 115.2, 47.8, 24.8. <sup>19</sup>F NMR (470 MHz DMSO-*d*<sub>6</sub>) δ -61.3. HR-MS (ESI) calculated for C<sub>18</sub>H<sub>9</sub>F<sub>3</sub>N<sub>3</sub>O<sub>3</sub>S [M + H]<sup>+</sup>: 414.1021, found: 414.1088. HPLC purity: 98%.

*1-(3,5-Dichlorophenyl)-3-(3-(pyrrolidin-1-ylsulfonyl)phenyl)urea (13)*. According to **GP-2**, using 1,3-dichloro-5-isocyanatobenzene (0.09 g, 0.48 mmol) to afford **13** after evaporation of the solvent as white solid (0.14 g, 77%). <sup>1</sup>H NMR (500 MHz, DMSO-*d*<sub>6</sub>) δ 9.4–9.1 (m, 2H), 8.1 (t, *J* = 1.8 Hz, 1H), 7.7–7.6 (m, 1H), 7.6–7.5 (m, 3H), 7.4 (d, *J* = 7.8 Hz, 1H), 7.2 (t, *J* = 1.8 Hz, 1H), 3.2–3.1 (m, 4H), 1.7–1.6 (m, 4H). <sup>13</sup>C NMR (126 MHz, DMSO-*d*<sub>6</sub>) δ 152.7, 142.5, 140.6, 137.1, 134.6, 130.4, 123, 121.7, 121.2, 117.2, 117.1, 48.3, 25.2.

HR-MS (ESI) calculated for C<sub>17</sub>H<sub>18</sub>Cl<sub>2</sub>N<sub>3</sub>O<sub>3</sub>S [M + H]<sup>+</sup>: 414.0368, found: 414.0430. HPLC purity: 99%

*1-(2-Fluoro-4-(trifluoromethyl)phenyl)-3-(3-(pyrrolidin-1-ylsulfonyl)phenyl)urea (14)*. According to **GP-2**, 2-fluoro-4-(trifluoromethyl)aniline (0.14 g, 0.79 mmol), to afford after purification by flash chromatography (cyclohexane/EtOAc = 1:1), **14** as white powder (0.04 g, 15 % yield). <sup>1</sup>H NMR (500 MHz, DMSO-*d*<sub>6</sub>) δ 9.6 (br s, 1H), 9.0 (br s, 1H), 8.4 (t, *J* = 8.3 Hz, 1H), 8.1 (s, 1H), 7.8–7.7 (m, 1H), 7.6–7.5 (m, 3H), 7.5–7.4 (m, 1H), 3.2–3.1 (m, 4H), 1.7–1.6 (m, 4H). <sup>13</sup>C NMR (126 MHz, DMSO-*d*<sub>6</sub>) δ 151.9, 151.7, 145.0, 139.7, 136.5, 129.9, 122.1, 121.9–121.6, 120.7, 120.1, 116.2, 47.7, 24.5. <sup>19</sup>F NMR (470 MHz DMSO-*d*<sub>6</sub>) δ -60.2, -127.7. HR-MS (ESI) calculated for C<sub>18</sub>H<sub>18</sub>F<sub>4</sub>N<sub>3</sub>O<sub>3</sub>S [M + H]<sup>+</sup>: 432.0927, found : 432.0995. HPLC purity: 99%.

*1-(Naphthalen-2-yl)-3-(3-(pyrrolidin-1-ylsulfonyl)phenyl)urea (15)*. According to **GP-2**, naphthalen-2-amine (0.1 g, 0.70 mmol), to afford after washing with MeOH (5x, 5mL), **15** as an off-white solid (0.02 g, 8% yield). <sup>1</sup>H NMR (500 MHz, DMSO-*d*<sub>6</sub>) δ 9.2 (s, 1 H), 9.0 (s, 1 H), 8.2 (s, 1 H), 8.1 (s, 1 H), 7.9 (br d, *J* = 8.85, 2 H), 7.8 (br d, *J* = 9.77, 1 H), 7.6 (d, *J* = 8.06, 1 H), 7.6 (t, *J* = 7.93, 1 H), 7.5 (dd, *J* = 8.77, 2.06, 1 H), 7.5 (t, *J* = 7.48, 1 H), 7.4–7.3 (m, 2 H), 3.2–3.1 (m, 4 H), 1.7–1.6 (m, 4 H). <sup>13</sup>C NMR (126 MHz, DMSO-*d*<sub>6</sub>) δ 152.7–152.8, 152.7, 140.7, 138.9–142.1, 137.2, 136.7, 133.8, 130, 129.4, 128.6, 127.6, 127.2, 126.6, 124.3, 122.3, 120.5, 120, 116.5, 114, 48, 24. HR-MS (ESI) calculated for C<sub>21</sub>H<sub>22</sub>N<sub>3</sub>O<sub>3</sub>S [M + H]<sup>+</sup>: 396.1304, found: 396.1364. HPLC purity: 99%.

*1-(4-Phenoxyphenyl)-3-(3-(pyrrolidin-1-ylsulfonyl)phenyl)urea (16)*. According to **GP-2**, using 4-phenoxyaniline (0.17 g, 0.94 mmol), to afford after purification with flash chromatography (cyclohexane/EtOAc = 7:3) **16** as a white solid (0.18 g, 44%). <sup>1</sup>H NMR (500 MHz, DMSO-*d*<sub>6</sub>) δ 9.1 (s, 1H), 8.8 (s, 1H), 8.1 (t, *J* = 2.0, 1H), 7.6 (ddd, *J* = 8.2, 2.3, 1.0, 1H), 7.5 (t, *J* = 7.9, 1H), 7.5–7.4 (m, 2H), 7.4–7.3 (m, 3H), 7.1 (t, *J* = 7.5, 1H), 7.0 (m, 4H), 3.2–3.1 (m, 4H), 1.7–1.6 (m, 4H). <sup>13</sup>C NMR (126 MHz, DMSO-*d*<sub>6</sub>) δ 158.1, 153.1, 151.4, 141.2, 137, 135.8, 130.4, 130.3, 123.3, 122.6, 120.9, 120.7, 120.2, 118.1, 116.8, 48.3, 25.2. HR-MS (ESI) calculated for C<sub>23</sub>H<sub>24</sub>N<sub>3</sub>O<sub>4</sub>S [M + H]<sup>+</sup>: 438.1409, found: 438.1474. HPLC purity: 99%.

*1-(3-(Morpholinomethyl)phenyl)-3-(3-(pyrrolidin-1-ylsulfonyl)phenyl)urea (17)*. According to **GP-2**, 3-(morpholinomethyl)aniline (0.1 g, 0.52 mmol), to afford after washing with MeOH (5x, 5 mL), **17** as a yellow crystalline powder (0.09 g, 31% yield). <sup>1</sup>H NMR (500 MHz, DMSO-*d*<sub>6</sub>) δ 9.1 (s, 1 H), 8.8 (s, 1 H), 8.1 (t, *J* = 1.91, 1 H), 7.6 (dd, *J* = 8.16, 1.14, 1 H), 7.5 (t, *J* = 7.93, 1 H), 7.4 (s, 1 H), 7.4–7.3 (m, 2 H), 7.3–7.2 (m, 1 H), 7.0–6.9 (m, 1 H), 3.6 (t, *J* = 4.50, 4 H), 3.4 (s, 2 H), 3.2–3.1 (m, 4 H), 2.4 (br s, 4 H), 1.7–1.6 (m, 4 H). <sup>13</sup>C NMR (126 MHz, DMSO-*d*<sub>6</sub>) δ 152.4, 140.6, 139.3, 138.6, 136.5, 129.8, 128.6, 122.8, 122.1, 120.2, 118.8, 117.2, 116.3, 66.2, 62.5, 53.2, 47.8, 24.7. HR-MS (ESI) calculated for C<sub>22</sub>H<sub>29</sub>N<sub>4</sub>O<sub>4</sub>S [M + H]<sup>+</sup>: 445.1831, found: 445.1899. HPLC purity: 98%.

*1-(3-((1H-Imidazol-1-yl)methyl)phenyl)-3-(3-(pyrrolidin-1-ylsulfonyl)phenyl)urea (18)*. According to **GP-2**, using 3-((1H-imidazol-1-yl)methyl)aniline (0.1 g, 0.58 mmol), to afford after washing with MeOH (5x, 5 mL), **18** as a white solid (0.01 g, 4% yield). <sup>1</sup>H NMR (500 MHz, DMSO-*d*<sub>6</sub>) δ 9.2

(br s, 1H), 8.9 (br s, 1H), 8.1 (s, 1H), 7.8 (s, 1H), 7.6–7.5 (m, 1H), 7.5 (t,  $J = 7.9$  Hz, 1H), 7.4–7.3 (m, 2H), 7.4–7.3 (m, 1H), 7.3 (t,  $J = 7.9$  Hz, 1H), 7.2–7.1 (m, 1H), 6.9 (s, 1H), 6.9–6.8 (m, 1H), 5.2 (s, 2H), 3.1 (br t,  $J = 6.6$  Hz, 4H), 1.7–1.6 (m, 4H).  $^{13}\text{C}$  NMR (126 MHz, DMSO- $d_6$ )  $\delta$  152.4, 140.5, 139.7, 138.4, 136.4, 129.7, 129, 122, 120.9, 120.1, 117.6, 117.1, 116.1, 49.4, 47.7, 24.6. HR-MS (ESI) calculated for  $\text{C}_{21}\text{H}_{24}\text{N}_5\text{O}_3\text{S}$  [M + H] $^+$ : 426.1522, found: 426.1582. HPLC purity: 98%.

*1-Methyl-1-(4-nitrophenyl)-3-(3-(pyrrolidin-1-ylsulfonyl)phenyl)urea* (**19**). To a flask containing triphosgene (0.08 g, 0.27 mmol), and DCM (2 mL) at 0 °C under argon atmosphere, a solution containing 3-((1H-imidazol-1-yl)methyl)aniline (0.13 g, 0.89 mmol), trimethylamine (247 mL, 1.78 mmol), and DCM (2 mL), was added. The resulting solution was stirred at room temperature for 2 h. To a different flask, *N*-methyl-4-nitroaniline (0.13 g, 0.89 mmol), sodium hydride (0.03 mg, 1.19 mmol), and DMF (2.5 mL) were added, the resulting solution was stirred at room temperature for two hours, after which, it was added dropwise to the solution containing triphosgene. The resulting mixture was stirred at room temperature for 1 h, next water was added and the mixture was extracted with EtOAc (5x, 20 mL). The combined organic layers were washed with saturated aqueous NaCl solution, dried over  $\text{MgSO}_4$ , filtered, concentrated *in vacuo*, and purified by column chromatography, ( $\text{CH}_2\text{Cl}_2/\text{MeOH}$ , 10/0  $\rightarrow$  9.5/0.5), and recrystallization ( $\text{CH}_2\text{Cl}_2/\text{diethyl ether}$ ), to afford **19** as a yellow solid (0.12 g, 32% yield).  $^1\text{H}$  NMR (500 MHz, DMSO- $d_6$ )  $\delta$  9.2 (s, 1H), 8.3–8.2 (m, 1H), 8.0 (t,  $J = 1.9$  Hz, 1H), 7.8 (dd,  $J = 8.1, 1.4$  Hz, 1H), 7.7–7.6 (m, 1H), 7.5 (t,  $J = 8.0$  Hz, 1H), 7.4 (d,  $J = 7.8$  Hz, 1H), 3.4 (s, 1H), 3.2–3.1 (m, 1H), 1.7–1.6 (m, 1H).  $^{13}\text{C}$  NMR (126 MHz, DMSO- $d_6$ )  $\delta$  154.7, 150.6, 143.9, 141.1, 136.7, 130, 125.4, 124.9, 124.3, 121.5, 118.8, 48.3, 37.4, 25.2. HR-MS (ESI) calculated for:  $\text{C}_{18}\text{H}_{21}\text{N}_4\text{O}_5\text{S}$  [M + H] $^+$ : 405.1154, found: 405.1214. HPLC purity: 99%.

*1-Methyl-3-(4-nitrophenyl)-1-(3-(pyrrolidin-1-ylsulfonyl)phenyl)urea* (**20**). A flask was charged with 3-(pyrrolidin-1-ylsulfonyl)aniline (0.1 g, 0.44 mmol), paraformaldehyde (0.09 g), and MeOH (5 mL). The resulting solution was stirred at room temperature for 2.5 h, after which,  $\text{NaBH}_4$  (0.03 g, 0.88 mmol) was added. The resulting mixture was stirred at 60 °C for 16 h, next, water (20 mL) was added, and the mixture was extracted with EtOAc (5x, 20 mL). The combined organic layers were washed with saturated aqueous NaCl solution, dried over  $\text{MgSO}_4$ , filtered, concentrated *in vacuo*, and purified by flash chromatography (EtOAc/petroleum benzene 3/7  $\rightarrow$  6/4) affording *N*-methyl-3-(pyrrolidin-1-ylsulfonyl)aniline (0.06 g, 0.25 mmol, 57% yield) which was added to a flask containing 1-isocyanato-4-nitrobenzene (0.07 g, 0.28 mmol), and DMF (5 mL). The solution was stirred at room temperature overnight, next, water (20 mL) was added, and the resulting mixture was extracted with EtOAc (5x, 20 mL). The combined organic layers were washed with saturated aqueous NaCl solution, dried over  $\text{MgSO}_4$ , filtered, concentrated *in vacuo*, purified by flash chromatography ( $\text{CH}_2\text{Cl}_2/\text{MeOH}$ , 10/0  $\rightarrow$  9.5/0.5), and recrystallized (MeOH,  $\text{CH}_2\text{Cl}_2$  and diethyl ether) to afford **20** as an off-white solid (0.02 g, 12% yield).  $^1\text{H}$  NMR (500

MHz, DMSO- $d_6$ )  $\delta$  9.2 (br s, 1H), 8.2 (d,  $J = 9.2$  Hz, 2H), 7.8–7.6 (m, 6H), 3.4 (s, 3H), 3.2–3.1 (m, 4H), 1.7–1.6 (m, 4H).  $^{13}\text{C}$  NMR (126 MHz, DMSO- $d_6$ )  $\delta$  154.5, 147.4, 144.9, 141.6, 137.2, 130.7 (d,  $J = 10.9$ ), 125.1, 124.9, 119.1, 48.3, 38.1, 25.1. HR-MS (ESI) calculated for:  $\text{C}_{18}\text{H}_{21}\text{N}_4\text{O}_5\text{S}$  [M + H] $^+$ : 405.1154, found: 405.1215. HPLC purity: 100%.

*1-(4-Nitrophenyl)-3-(3-(pyrrolidin-1-ylsulfonyl)phenyl)thiourea* (**21**). To 3-(pyrrolidin-1-ylsulfonyl)aniline (0.03 g, 0.11 mmol) dissolved in DCM (5 mL) was added 1-isothiocyanato-4-nitrobenzene (0.02 g, 0.11 mmol) at 0 °C. The reaction was then stirred at room temperature for 2 days. The reaction was quenched by the addition of saturated aqueous solution of  $\text{NaHCO}_3$  (20 mL), and extracted with DCM. The organic solvent was dried over  $\text{MgSO}_4$ , filtered, and then removed *in vacuo* and the reaction was purified using preparative HPLC affording **21** (0.02 g, 35% yield).  $^1\text{H}$  NMR (500 MHz, DMSO- $d_6$ )  $\delta$  9.0 (s, 1H), 7.9 (t,  $J = 1.8$  Hz, 1H), 7.8 (d,  $J = 8.5$  Hz, 2H), 7.8 (dd,  $J = 8.2, 1.3$  Hz, 1H), 7.6 (d,  $J = 8.4$  Hz, 2H), 7.5 (t,  $J = 8.0$  Hz, 1H), 7.4–7.3 (m, 1H), 3.2–3.1 (m, 4H), 1.7–1.62 (m, 4H).  $^{13}\text{C}$  NMR (126 MHz, DMSO- $d_6$ )  $\delta$  153.7, 145.4, 140.5, 136, 129.5, 127.3, 126.5, 123.9, 121, 118.4, 80.1, 75.1, 47.9, 24.7. HR-MS (ESI) calculated for  $\text{C}_{17}\text{H}_{19}\text{N}_4\text{O}_4\text{S}_2$  [M + H] $^+$ : 407.0770, found: 407.0839. HPLC purity: 95%.

*N,N-Dimethyl-3-(3-(4-nitrophenyl)ureido)benzenesulfonamide* (**22**). According to **GP-3** using, 3-amino-*N,N*-dimethylbenzenesulfonamide (0.1 g, 0.5 mmol), and DCM (10 mL), to afford after filtration of the precipitate, **22** as a white solid (0.09 g, 49% yield).  $^1\text{H}$  NMR (500 MHz, DMSO- $d_6$ )  $\delta$  9.6–9.3 (m, 2H), 8.2–8.1 (m, 2H), 8.1 (t,  $J = 1.8$  Hz, 1H), 7.8–7.7 (m, 2H), 7.6 (dd,  $J = 7.9, 1.5$  Hz, 1H), 7.6 (t,  $J = 7.9$  Hz, 1H), 7.4 (d,  $J = 7.8$  Hz, 1H), 2.7–2.6 (m, 6H).  $^{13}\text{C}$  NMR (126 MHz, DMSO- $d_6$ )  $\delta$  152.5, 146.6, 141.7, 140.5, 135.7, 130.4, 125.6, 123.2, 121.7, 118.3, 117.5, 38.1. HR-MS (ESI) calculated for  $\text{C}_{15}\text{H}_{17}\text{N}_4\text{O}_5\text{S}$  [M + H] $^+$ : 365.0841, found: 365.0915. HPLC purity: 99%.

*N,N-diethyl-3-(3-(4-nitrophenyl)ureido)benzenesulfonamide* (**23**). According to **GP-3** using, 3-amino-*N,N*-diethylbenzenesulfonamide (0.114 g, 0.5 mmol), and DCM (10 mL), to afford after filtration of the precipitate, **23** as a yellow solid (0.11 g, 58% yield).  $^1\text{H}$  NMR (500 MHz, DMSO- $d_6$ )  $\delta$  9.4 (br s, 2H), 8.2–8.1 (m,  $J = 9.2$  Hz, 2H), 8.1–8.0 (m, 1H), 7.8–7.7 (m, 2H), 7.6 (dd,  $J = 8.2, 1.0$  Hz, 1H), 7.5 (t,  $J = 7.9$  Hz, 1H), 7.4 (d,  $J = 7.8$  Hz, 1H), 3.2 (q,  $J = 7.2$  Hz, 4H), 1.1 (t,  $J = 7.2$  Hz, 6H).  $^{13}\text{C}$  NMR (126 MHz, DMSO- $d_6$ )  $\delta$  152.5, 146.6, 141.7, 140.8, 140.5, 130.4, 125.6, 122.7, 120.8, 118.3, 116.7, 42.3, 14.6. HR-MS (ESI) calculated for  $\text{C}_{17}\text{H}_{21}\text{N}_4\text{O}_5\text{S}$  [M + H] $^+$ : 393.1154, found: 393.1221. HPLC purity: 99%.

*1-(4-Nitrophenyl)-3-(3-(piperidin-1-ylsulfonyl)phenyl)urea* (**24**). According to **GP-3** using, 3-(piperidin-1-ylsulfonyl)aniline (0.120 g, 0.5 mmol), and DCM (10 mL), to afford after filtration of the precipitate, **24** as an off-white solid (0.12 g, 55% yield).  $^1\text{H}$  NMR (500 MHz, DMSO- $d_6$ )  $\delta$  9.6–9.3 (m, 2H), 8.2–8.1 (m, 2H), 8.1–8.0 (m, 1H), 7.8–7.7 (m, 2H), 7.7 (dd,  $J = 7.9, 1.6$  Hz, 1H), 7.6 (t,  $J = 7.9$  Hz, 1H), 7.4–7.3 (m, 1H), 2.9–2.8 (m, 4H), 1.6–1.5 (m, 4H), 1.4–1.3 (m, 2H).  $^{13}\text{C}$  NMR (126 MHz, DMSO- $d_6$ )  $\delta$  152.5, 146.5, 141.7, 140.5, 136.6, 130.4, 125.6, 123.1, 121.6, 118.3, 117.3, 47.1, 25.2,



23.3. HR-MS (ESI) calculated for  $C_{18}H_{21}N_4O_5S$  [M + H]<sup>+</sup>: 405.1154, found: 405.1213. HPLC purity: 99%.

1-(3-(Morpholinosulfonyl)phenyl)-3-(4-nitrophenyl)urea (**25**). According to GP-3 using, 3-morpholinosulfonyl aniline (0.12 g, 0.5 mmol), and  $CH_2Cl_2$  (5 mL), to afford after filtration of the precipitate, **25** as a white powder (0.06 g, 31% yield). <sup>1</sup>H NMR (500 MHz, DMSO-*d*<sub>6</sub>) δ 9.6–9.3 (m, 2H), 8.2–8.1 (m, 2H), 8.1–8.0 (m, 1H), 7.8–7.7 (m, 2H), 7.7–7.6 (m, 1H), 7.6–7.5 (m, 1H), 7.4 (d, *J* = 7.6 Hz, 1H), 3.7–3.6 (m, 4H), 2.9–2.8 (m, 4H). <sup>13</sup>C NMR (126 MHz, DMSO-*d*<sub>6</sub>) δ 152.6, 141.7, 140.6, 135.4, 130.5, 125.6, 123.5, 121.8, 118.3, 117.5, 65.8, 46.4. HR-MS (ESI) calculated for  $C_{17}H_{19}N_4O_6S$  [M + H]<sup>+</sup>: 407.0947, found: 407.1006. HPLC purity: 99%.

1-(4-Nitrophenyl)-3-(3-(phenylsulfonyl)phenyl)urea (**26**). According to GP-3 3-(pyrrolidin-1-ylsulfonyl)aniline (0.16 g, 0.69 mmol) to afford after purification by flash chromatography ( $CH_2Cl_2/MeOH$ , 10/0 → 9.5/0.5), and washing the residue with MeOH, and  $CH_2Cl_2$ , **26** as a yellow powder (0.08 g, 28% yield). <sup>1</sup>H NMR (500 MHz, DMSO-*d*<sub>6</sub>) δ 9.7–9.6 (m, 1H), 9.5–9.4 (m, 1H), 8.3–8.2 (m, 1H), 8.2–8.1 (m, 2H), 8.0–7.9 (m, 2H), 7.8–7.7 (m, 3H), 7.7–7.5 (m, 5H). <sup>13</sup>C NMR (126 MHz, DMSO-*d*<sub>6</sub>) δ 152.5, 146.5, 142.1, 141.8, 141.5, 140.8, 134.3, 130.9, 130.3, 127.8, 125.6, 123.8, 121.5, 118.5, 118.3, 117. HR-MS (ESI) calculated for:  $C_{19}H_{16}N_3O_5S$  [M + H]<sup>+</sup>: 398.0732, found: 398.0800. HPLC purity: 98%.

1-(4-Fluoro-3-(morpholinosulfonyl)phenyl)-3-(4-nitrophenyl)urea (**27**). According to GP-3 using, 4-fluoro-3-(morpholinosulfonyl)aniline (0.08 g, 0.46 mmol), to afford after purification by flash chromatography ( $CH_2Cl_2/MeOH$ , 10/0 → 9.5/0.5), and washing the residue with MeOH, **27** as a yellow powder (0.05 g, 23 % yield). <sup>1</sup>H NMR (500 MHz, DMSO-*d*<sub>6</sub>) δ 9.5 (br s, 1H), 9.3 (br s, 1H), 8.2–8.1 (m, 2H), 8.1 (dd, *J* = 6.0, 2.7 Hz, 1H), 7.8–7.7 (m, 3H), 7.5 (t, *J* = 9.5 Hz, 1H), 3.7–3.6 (m, 4H), 3.1–3.0 (m, 4H). <sup>13</sup>C NMR (126 MHz, DMSO-*d*<sub>6</sub>) δ 154.9, 152.9, 152.5, 146.5, 141.7, 136.4, 126, 125.6, 123.7, 120.6, 118.7, 118.5, 118.3, 66, 46. <sup>19</sup>F NMR (470 MHz DMSO-*d*<sub>6</sub>) δ -116.4. HR-MS (ESI) calculated for:  $C_{17}H_{18}FN_4O_6S$  [M + H]<sup>+</sup>: 425.0853, found: 425.0913. HPLC purity: 96%.

1-(4-Chloro-3-(morpholinosulfonyl)phenyl)-3-(4-nitrophenyl)urea (**28**). According to GP-3 using, 4-chloro-3-(morpholinosulfonyl)aniline (0.1 g, 0.36 mmol), to afford after filtration, and washing (MeOH,  $CH_2Cl_2$  and diethyl ether), **28** as yellow solid (0.01g, 7% yield). <sup>1</sup>H NMR (500 MHz, DMSO-*d*<sub>6</sub>) δ 9.7–9.4 (m, 2H), 8.2 (d, *J* = 2.4 Hz, 1H), 8.3–8.2 (m, 2H), 7.8–7.7 (m, 3H), 7.7–7.6 (m, 1H), 3.7–3.6 (m, 4H), 3.2–3.1 (m, 4H). <sup>13</sup>C NMR (126 MHz, DMSO-*d*<sub>6</sub>) δ 151.96, 145.98, 141.33, 138.69, 134.93, 132.74, 125.12, 123.85, 123.31, 120.89, 117.90, 65.72, 45.74. HR-MS (ESI) calculated for:  $C_{17}H_{18}ClN_4O_6S$  [M + H]<sup>+</sup>: 441.0557, found: 441.0623. HPLC purity: 99%

1-(4-Methyl-3-(morpholinosulfonyl)phenyl)-3-(4-nitrophenyl)urea (**29**). According to GP-3 using, 4-methyl-3-(morpholinosulfonyl)aniline (0.1 g, 39 mmol), affording after purification by flash chromatography ( $CH_2Cl_2/MeOH$ , 10/0 → 9.5/0.5), and recrystallization (MeOH,  $CH_2Cl_2$ , and diethyl ether), **29** as a white solid (0.02 g, 9% yield). <sup>1</sup>H NMR (500 MHz, DMSO-*d*<sub>6</sub>) δ 9.5 (br s, 1H), 9.28 (br s, 1H), 8.3–8.2 (m, 2H), 8.1 (d, *J* = 2.4 Hz, 1H),

7.8–7.7 (m, 2H), 7.6 (dd, *J* = 8.2, 2.3 Hz, 1H), 7.4 (d, *J* = 8.4 Hz, 1H), 3.7–3.6 (m, 4H), 3.4 (s, 9H), 3.1–3.0 (m, 4H). <sup>13</sup>C NMR (126 MHz, DMSO-*d*<sub>6</sub>) δ 152.5, 146.7, 141.6, 137.9, 135.2, 134, 131.3, 125.7, 123.5, 119.8, 118.2, 66, 45.8, 20.2. HR-MS (ESI) calculated for:  $C_{18}H_{21}N_4O_6S$  [M + H]<sup>+</sup>: 421.1104, found: 421.1174. HPLC purity: 99%.

1-(4-Fluoro-3-(pyrrolidin-1-ylsulfonyl)phenyl)-3-(4-nitrophenyl)urea (**30**). According to GP-4 using, 1-(2-fluoro-5-nitrophenyl)sulfonylpyrrolidine (0.1 g, 0.42 mmol), to afford after purification by preparative RP-HPLC **30** as an orange solid (0.01 g, 6% yield). <sup>1</sup>H NMR (500 MHz, DMSO-*d*<sub>6</sub>): δ 10.2–9.8 (m, 1H), 8.8–8.6 (m, 1H), 8.2 (d, *J* = 9.2 Hz, 2H), 7.8 (d, *J* = 2.3 Hz, 1H), 7.7 (d, *J* = 9.2 Hz, 2H), 7.7 (d, *J* = 2.3 Hz, 1H), 7.0 (d, *J* = 9.0 Hz, 1H), 3.5–3.4 (m, 4H), 1.9–1.8 (m, 4H). <sup>13</sup>C NMR (126 MHz, DMSO-*d*<sub>6</sub>): δ 153.1, 150.7, 146.6, 140.7, 129.3, 127.1, 124.9, 123.4, 117.3, 115.2, 49.8, 24.9. <sup>19</sup>F NMR (470 MHz DMSO-*d*<sub>6</sub>) δ -73.5. HR-MS (ESI) calculated for:  $C_{17}H_{17}FN_4O_5S$  [M + H]<sup>+</sup>: 409.0904, found: 409.0967. HPLC purity: 96%.

1-(2-Fluoro-5-(pyrrolidin-1-ylsulfonyl)phenyl)-3-(4-nitrophenyl)urea (**31**). According to GP-4 using, 4-fluoro-3-nitrobenzenesulfonyl chloride (0.1 g, 0.42 mmol), to afford after purification by preparative RP-HPLC **31** as a gray solid (0.01 g, 5% yield). <sup>1</sup>H NMR (500 MHz, DMSO-*d*<sub>6</sub>): δ 9.6 (br s, 1H), 9.2 (br s, 1H), 8.2 (d, *J* = 2.4 Hz, 1H), 8.2 (d, *J* = 9.2 Hz, 2H), 7.7 (d, *J* = 9.2 Hz, 2H), 7.7 (dd, *J* = 9.2, 2.3 Hz, 1H), 7.3 (d, *J* = 9.2 Hz, 1H), 3.4–3.3 (m, 4H), 2.0–1.9 (m, 4H). <sup>13</sup>C NMR (126 MHz, DMSO-*d*<sub>6</sub>): δ 152.1, 146.2, 144.9, 141.0, 130.3, 128.4, 125.0, 120.7, 120.0, 117.5, 51.8, 25.1. <sup>19</sup>F NMR (470 MHz DMSO-*d*<sub>6</sub>) δ -115.9. HR-MS (ESI) calculated for:  $C_{17}H_{17}FN_4O_5S$  [M + H]<sup>+</sup>: 409.0904, found: 409.0967. HPLC purity: 98.

1-(2-Chloro-5-(pyrrolidin-1-ylsulfonyl)phenyl)-3-(4-nitrophenyl)urea (**32**). According to GP-4 using, 4-chloro-3-nitrobenzenesulfonyl chloride (0.15 g, 0.59 mmol), to afford after purification by preparative RP-HPLC **32** as a yellow solid (0.02 g, 7% yield). <sup>1</sup>H NMR (500 MHz, DMSO-*d*<sub>6</sub>): δ 10.3–10.1 (m, 1H), 8.9–8.7 (m, 1H), 8.7 (d, *J* = 2.0 Hz, 1H), 8.2 (d, *J* = 9.2 Hz, 2H), 7.8 (d, *J* = 8.4 Hz, 1H), 7.7 (d, *J* = 9.2 Hz, 2H), 7.5 (dd, *J* = 8.4, 2.0 Hz, 1H), 3.2–3.1 (m, 4H), 1.7–1.6 (m, 4H). <sup>13</sup>C NMR (126 MHz, DMSO-*d*<sub>6</sub>): δ 152.1, 146.0, 142.0, 136.7, 135.9, 130.8, 126.8, 125.7, 122.5, 119.8, 118.0, 118.3, 48.4, 25.2. HR-MS (ESI) calculated for:  $C_{17}H_{17}ClN_4O_5S$  [M + H]<sup>+</sup>: 425.0608, found: 425.0686. HPLC purity: 97%.

1-(2-Methyl-5-(pyrrolidin-1-ylsulfonyl)phenyl)-3-(4-nitrophenyl)urea (**33**). According to GP-4 using, 4-methyl-3-nitrobenzenesulfonyl chloride (0.15 g, 0.59 mmol), to afford after purification by preparative RP-HPLC **33** as a yellow solid (0.07 g, 28% yield). <sup>1</sup>H NMR (500 MHz, DMSO-*d*<sub>6</sub>): δ 10.0–9.7 (m, 1H), 8.4 (d, *J* = 1.7 Hz, 1H), 8.2 (d, *J* = 9.2 Hz, 2H), 7.7 (d, *J* = 9.2 Hz, 2H), 7.5 (d, *J* = 7.9 Hz, 1H), 7.4 (dd, *J* = 8.7, 2.0 Hz, 1H), 3.2–3.1 (m, 4H), 2.4 (s, 3H), 1.7–1.6 (m, 4H). <sup>13</sup>C NMR (126 MHz, DMSO-*d*<sub>6</sub>): δ 151.9, 145.9, 141.0, 137.4, 133.7, 132.5, 130.9, 125.1, 125.0, 121.4, 118.8, 117.8, 117.4, 47.6, 24.5, 17.8. HR-MS (ESI) calculated for:  $C_{18}H_{20}N_4O_5S$  [M + H]<sup>+</sup>: 405.1154, found: 405.1219. HPLC purity: 98%.

1-(2,5-Dimethyl-3-(pyrrolidin-1-ylsulfonyl)phenyl)-3-(4-nitrophenyl)urea (**34**). According to GP-4 using, 2,5-dimethyl-3-nitrobenzenesulfonyl chloride (0.15 g, 0.60 mmol), to afford after purification by preparative RP-HPLC

**34** as a yellow solid (0.09 g, 37% yield).  $^1\text{H}$  NMR (500 MHz, DMSO- $d_6$ ):  $\delta$  9.9–9.7 (m, 1H), 8.5–8.2 (m, 1H), 8.2 (d,  $J$  = 9.2 Hz, 2H), 7.8–7.7 (m, 1H), 7.7 (d,  $J$  = 9.2 Hz, 2H), 7.5–7.4 (m, 1H), 3.2 (m, 4H), 2.4 (s, 3H), 2.4 (s, 3H), 1.9–1.8 (m, 4H).  $^{13}\text{C}$  NMR (126 MHz, DMSO- $d_6$ ):  $\delta$  152.4, 146.5, 141.2, 138.7, 137.6, 135.6, 128.3, 126.2, 125.4, 125.0, 117.6, 47.4, 25.2, 20.9, 14.1. HR-MS (ESI) calculated for:  $\text{C}_{19}\text{H}_{22}\text{N}_4\text{O}_5\text{S}$  [ $\text{M} + \text{H}$ ] $^+$ : 419.1311, found: 419.1373. HPLC purity: 100%.

**1-(4-Nitrophenyl)-3-(4-(pyrrolidin-1-yl)-3-(pyrrolidin-1-ylsulfonyl)phenyl)urea (35)**. To a flask containing acetonitrile (1.5 mL), trimethylamine (0.12 g, 1.17 mmol), and pyrrolidine (0.04 g, 0.59 mmol) at room temperature, 2-chloro-5-nitrobenzenesulfonyl chloride (0.15 g, 0.59 mmol) was added. Next the resulting solution was stirred at room temperature for 5 min, after which, the solvent was evaporated. To the residue, EtOH (5.4 mL, 0.1 mmol), an aqueous solution of  $\text{NH}_4\text{Cl}$  at a concentration of 166 mM in water (2.0 mL, 0.34 mmol), and Fe powder (0.19 g, 3.44 mmol) were added, the resulting reaction mixture was stirred at 80 °C for 2.5 h. Next, the organic solvent was evaporated *in vacuo*, water (20 mL) was added, and the solution was extracted with EtOAc (3x, 20 mL). The combined organic layers were dried over  $\text{MgSO}_4$ , filtered, and concentrated *in vacuo*. Subsequent, the residue was solubilized with DMF (2 mL), and 1-isocyanato-4-nitrobenzene (0.14 g, 0.86 mmol) was added. The resulting reaction mixture was stirred at room temperature for 1 h, after which, DMF was removed on reduced pressure, and the residue was purified using preparative RP-HPLC to yield **35** as a yellow solid (0.01 g, 13% yield).  $^1\text{H}$  NMR (500 MHz, DMSO- $d_6$ ):  $\delta$  9.6–9.3 (m, 1H), 9.3–9.0 (m, 1H), 8.2 (d,  $J$  = 9.2 Hz, 2H), 8.0 (d,  $J$  = 2.6 Hz, 1H), 7.7 (d,  $J$  = 9.2 Hz, 1H), 7.6 (dd,  $J$  = 8.9, 2.6 Hz, 1H), 7.4 (d,  $J$  = 8.9 Hz, 1H), 3.3–3.2 (m, 4H), 3.2–3.1 (m, 4H), 1.9–1.8 (m, 4H), 1.8–1.7 (m, 4H).  $^{13}\text{C}$  NMR (126 MHz, DMSO- $d_6$ ):  $\delta$  152.0, 146.3, 144.3, 141.0, 134.1, 133.6, 125.1, 123.8, 123.4, 120.8, 117.6, 53.6, 47.7, 25.4, 24.2. HR-MS (ESI) calculated for:  $\text{C}_{21}\text{H}_{25}\text{N}_5\text{O}_5\text{S}$  [ $\text{M} + \text{H}$ ] $^+$ : 460.1576, found: 460.1653. HPLC purity: 99%.

**1-(4-Nitrophenyl)-3-(2-(pyrrolidin-1-yl)-5-(pyrrolidin-1-ylsulfonyl)phenyl)urea (36)**. To a flask containing acetonitrile (1.5 mL), trimethylamine (0.12 g, 1.17 mmol), and pyrrolidine (0.04 g, 0.59 mmol) at room temperature, 4-chloro-3-nitrobenzenesulfonyl chloride (0.15 g, 0.59 mmol) was added. Next the resulting solution was stirred at room temperature for 5 min, after which, the solvent was evaporated. To the residue, EtOH (5.4 mL, 0.1 mmol), an aqueous solution of  $\text{NH}_4\text{Cl}$  at a concentration of 166 mM in water (2.0 mL, 0.34 mmol), and Fe powder (0.19 g, 3.44 mmol) were added, the resulting reaction mixture was stirred at 80 °C for 2.5 h. Next, the organic solvent was evaporated *in vacuo*, water (20 mL) was added, and the solution was extracted with EtOAc (3x). The combined organic layers were dried over  $\text{MgSO}_4$ , filtered, and concentrated *in vacuo*. Subsequently, the residue was solubilized with DMF (2 mL) and 1-isocyanato-4-nitrobenzene (0.14 g, 0.86 mmol) was added. The resulting reaction mixture was stirred at room temperature for 1 h, after which, DMF was removed on reduced pressure and the residue was purified using preparative RP-HPLC to yield **36** as a yellow solid (0.02 g, 9% yield)  $^1\text{H}$  NMR (500

13

MHz, DMSO- $d_6$ ):  $\delta$  9.8 (br s, 1H), 8.2 (br s, 1H), 8.2 (d,  $J$  = 9.2 Hz, 2H), 7.8 (d,  $J$  = 2.1 Hz, 1H), 7.7 (d,  $J$  = 9.3 Hz, 2H), 7.4 (dd,  $J$  = 8.7, 2.3 Hz, 1H), 7.0 (d,  $J$  = 8.9 Hz, 1H), 3.3 (m, 4H), 3.1–3.0 (m, 4H), 2.0–1.9 (m, 4H), 1.7–1.6 (m, 4H).  $^{13}\text{C}$  NMR (126 MHz, DMSO- $d_6$ ):  $\delta$  152.9, 147.4, 146.7, 141.1, 126.0, 125.7, 125.3, 125.2, 124.5, 117.6, 115.8, 50.2, 47.9, 25.0, 24.7. HR-MS (ESI) calculated for:  $\text{C}_{21}\text{H}_{25}\text{N}_5\text{O}_5\text{S}$  [ $\text{M} + \text{H}$ ] $^+$ : 460.1576, found: 460.1652. HPLC purity: 97%.

**Photometric *in vitro* assay.** Dilution series (1:2) of inhibitors in DMSO covered the concentration range of approximately 200–0.01  $\mu\text{M}$ . After finishing the dilution series, the final volume of compound solution in DMSO per well was 3  $\mu\text{L}$ . For the IspD assay, 30  $\mu\text{L}$  aliquots of a solution containing 100 mM Tris-HCl, pH 7.6, 0.02%  $\text{NaN}_3$ , 1 mM MEP and 1 mM CTP were added to microplate wells preloaded with 3  $\mu\text{L}$  of DMSO containing test compounds. The reaction was started by addition of 27  $\mu\text{L}$  aliquots of buffer: 100 mM Tris-HCl, pH 7.6, containing 10 mM  $\text{MgCl}_2$ , 60 mM KCl, 10 mM dithiothreitol, 0.02%  $\text{NaN}_3$ , 1 mM NADH, 2 mM phosphoenolpyruvate, 2 mM ATP, 1 U  $\text{mL}^{-1}$  pyruvate kinase, 1 U  $\text{mL}^{-1}$  lactate dehydrogenase, 1.5 U  $\text{mL}^{-1}$  *E. coli* IspE, 0.01  $\mu\text{M}$  PflspD. The reaction was monitored photometrically (340 nm) at room temperature for 30 – 60 min on a plate reader (Spectramax M2, Molecular Devices, Biberach an der Riss, Germany). Initial rates were estimated using Softmax Pro 6.1 software (Molecular Devices, Biberach an der Riss, Germany).  $\text{IC}_{50}$  values were determined with a nonlinear regression method using the program Dynafit.<sup>19</sup>

**Whole-cell assay.** *PfNF54* wild type parasites cultured in RPMI 1640 medium supplemented with 25 mM HEPES, 24 mM sodium bicarbonate (pH 7.3), 0.36 mM hypoxanthine, 100  $\mu\text{g}/\text{mL}$  neomycin and 0.5% Albumax II were used to test for compound activity on parasite multiplication using a [ $^3\text{H}$ ]-hypoxanthine incorporation assay.<sup>20</sup> Compounds were dissolved in DMSO (10 mM), diluted in hypoxanthine-free culture medium and titrated in duplicate over a 64-fold range (6 step twofold dilutions) in 96 well plates. 100  $\mu\text{L}$  Asexual parasite culture (prepared in hypoxanthine-free medium) were added to each well and mixed with the compound to obtain a final haematocrit of 1.25% and a final parasitemia of 0.3%. After incubation for 48 h, 0.25  $\mu\text{Ci}$  of [ $^3\text{H}$ ]-hypoxanthine was added per well and plates were incubated for an additional 24 h. Parasites were then harvested onto glass-fiber filters using a Microbeta FilterMate cell harvester (Perkin Elmer, Waltham, US), and radioactivity was counted using a MicroBeta2 liquid scintillation counter (Perkin Elmer, Waltham, US). The results were recorded and expressed as a percentage of the untreated controls. Fifty percent inhibitory concentrations ( $\text{EC}_{50}$ ) were estimated by linear interpolation.<sup>21</sup>

#### LC-MS based *in vitro* assay.

Dilution series (1:2) of inhibitors in DMSO covered the concentration range of approximately 200–0.01  $\mu\text{M}$ . After finishing the dilution series, the final volume of compound solution in DMSO per well was 2.0  $\mu\text{L}$ . During the assay, the following buffer was used: 100 mM Tris-HCl pH 7.6, 1 mM DTT. To start the assay, aliquots of buffer (49  $\mu\text{L}$ ) containing: 306.1  $\mu\text{M}$  CTP, 2.0 mM  $\text{MgCl}_2$  and 0.1  $\mu\text{M}$



PflspD, were added to a 96-well plate (Nunc V). Next 2  $\mu\text{L}$  of the inhibitor dilutions (in DMSO) are added and the plate is allowed to incubate at 37  $^{\circ}\text{C}$  for 10 min. Then another 49  $\mu\text{L}$  of buffer containing 306.1  $\mu\text{M}$  MEP was added to start the reaction. The plates were incubated at 37  $^{\circ}\text{C}$  for 40 min, after which, the protein was denaturated by heating up the plate to 95  $^{\circ}\text{C}$  for 5 min. The plate was then centrifuged at 4000 rpm at 4  $^{\circ}\text{C}$  for 5 min to precipitate all solids present in the solution. To another 96-well plate, 190  $\mu\text{L}$  of ice cold 3:1:1 ACN, isopropanol, water mixture was added. Thereafter, 10  $\mu\text{L}$  of each of the supernatants from the assay plate were added. The plate was centrifuged again at 4000 rpm at 4  $^{\circ}\text{C}$  for 5 min, after which, 50  $\mu\text{L}$  of the supernatant was transferred to a plate capable to measured in the MS and covered with a silicon cover. LC-MS conditions and data analysis methods we used were described above.

**Determination of enzyme kinetics.** A volume of 80  $\mu\text{L}$  Buffer A containing 100mM Tris-HCl pH 7.6, 1 mM DTT, 1 mM  $\text{MgCl}_2$ , 50 nM PflspD were added to well A<sub>1</sub> 96-well plate while 50  $\mu\text{L}$  were added to the rest of the wells. A volume of 20  $\mu\text{L}$  of 10mM CTP was added to the first well, then a serial dilution was conducted by moving 50  $\mu\text{L}$ . To start the reaction, we then added on buffer A 50  $\mu\text{L}$  of Buffer B containing 100mM Tris-HCl pH 7.6, 1 mM DTT, and 1 mM MEP. The assay plate was incubated at 37  $^{\circ}\text{C}$  for 40 min, after which, the protein was denaturated by heating up the plate to 95  $^{\circ}\text{C}$  for 5 min. The plate was then centrifuged at 4000 rpm at 4  $^{\circ}\text{C}$  for 5 min to precipitate the protein. To another 96-well plate, 190  $\mu\text{L}$  of ice cold 3:1:1 ACN, isopropanol, water mixture was added containing 100 nM 4-methyl-1-oxo-1-(p-tolylamino)pentane-2-sulfonic acid, adenylyl-imidodiphosphate and adenosine-5'-[( $\alpha,\beta$ )-methylene]triphosphate as internal standard.<sup>15</sup> Thereafter, 10  $\mu\text{L}$  of each of the supernatants from the assay plate were added to the plate containing the mixture with our internal standard. The plate was centrifuged again at 4000 rpm at 4  $^{\circ}\text{C}$  for 5 min, after which, 50  $\mu\text{L}$  of the supernatant was transferred to an LC-MS plate and closed with a silicon cover. LC-MS conditions and data analysis methods we used were described above. The peak area for each conditions were used to calculate the Michaelis–Menten kinetic parameters using Graphpad Prism v 9. Measurements were performed in duplicates, repeated at least two times from two to three independent experiments.

**Determination of mode of inhibition of 10.** Dilution series (1:2) of inhibitors in DMSO covered the concentration range of approximately 200–0.01  $\mu\text{M}$ . After finishing the dilution series, the final volume of compound solution in DMSO per well was 2.0  $\mu\text{L}$ . During the assay, the following buffer was used: 100 mM Tris-HCl pH 7.6, 1 mM DTT. To study the inhibition mode against CTP, aliquots of buffer (49  $\mu\text{L}$ ) containing: 0, 37.5, 75, 125, 250,

500  $\mu\text{M}$  CTP, 2.0 mM  $\text{MgCl}_2$  and 0.1  $\mu\text{M}$  PflspD, were added to a 96-well plate (Nunc V). Next 2  $\mu\text{L}$  of the inhibitor dilutions (in DMSO) are added and the assay plate was incubated at 37  $^{\circ}\text{C}$  for 10 min. Then another 49  $\mu\text{L}$  of buffer containing 500  $\mu\text{M}$  MEP was added to start the reaction. To study the Mode of inhibition toward MEP, similar steps were followed as in case of CTP with using 0, 37.5, 75, 125, 250, 500  $\mu\text{M}$  MEP and 500  $\mu\text{M}$  CTP The assay plate was incubated at 37  $^{\circ}\text{C}$  for 40 min, after which, the protein was denaturated by heating up the plate to 95  $^{\circ}\text{C}$  for 5 min. The assay plate was then centrifuged at 4000 rpm at 4  $^{\circ}\text{C}$  for 5 min to precipitate the protein. To another 96-well plate, 190  $\mu\text{L}$  of ice cold 3:1:1 ACN, isopropanol, water mixture was added containing 100 nM 4-methyl-1-oxo-1-(p-tolylamino)pentane-2-sulfonic acid as internal standard.<sup>15</sup> Thereafter, 10  $\mu\text{L}$  of each of the supernatants from the assay plate were added to the plate containing the mixture with our internal standard. The plate was centrifuged again at 4000 rpm at 4  $^{\circ}\text{C}$  for 5 min, after which, 50  $\mu\text{L}$  of the supernatant was transferred to an LC-MS plate and closed with a silicon cover. LC-MS conditions and data analysis methods we used were described above.

**Metabolic Stability in Liver S<sub>9</sub> Fractions.** For the evaluation of combined phase I and phase II metabolic stability, the compound (1  $\mu\text{M}$ ) was incubated with 1 mg/mL pooled mouse liver S<sub>9</sub> fraction (Xenotech, Kansas City, USA) or human liver S<sub>9</sub> fraction (Corning, USA), 2 mM NADPH, 1 mM UDPGA, 10 mM  $\text{MgCl}_2$ , 5 mM GSH and 0.1 mM PAPS at 37  $^{\circ}\text{C}$  for 240 min. The metabolic stability of testosterone, verapamil and ketoconazole were determined in parallel to confirm the enzymatic activity of mouse S<sub>9</sub> fractions, for human S<sub>9</sub> testosterone, diclofenac and propranolol were used. The incubation was stopped after defined time points by precipitation of aliquots of S<sub>9</sub> enzymes with 2 volumes of cold acetonitrile containing internal standard (150 nM diphenhydramine). Samples were stored on ice until the end of the incubation and precipitated protein was removed by centrifugation (4  $^{\circ}\text{C}$ , 15 min, 4,000 g). Concentration of the remaining test compound at the different time points was analyzed by HPLC-MS/MS (TSQ Quantum Access MAX, Thermo Fisher, Dreieich, Germany) and used to determine half-life ( $t_{1/2}$ ).

**Stability in Mouse and Human Plasma.** To determine stability in mouse plasma, the compound (1  $\mu\text{M}$ ) was incubated with pooled CD-1 mouse or human plasma (Neo Biotech, Nanterre, France). Samples were taken at defined time points by mixing aliquots with 4 volumes of acetonitrile containing internal standard (125 nM diphenhydramine). Samples were stored on ice until the end of the incubation and precipitated protein was removed by centrifugation (4  $^{\circ}\text{C}$ , 15 min, 4,000 g, 2 centrifugation steps). Concentration of the remaining test compound at the different time points was analyzed by HPLC-MS/MS (TSQ Quantum Access MAX, Thermo Fisher, Dreieich, Germany). The plasma stability of

procain, propantheline and diltiazem were determined in parallel to confirm the enzymatic activity.

**Pharmacokinetic (PK) studies.** For pharmacokinetic experiments, outbred male CD-1 mice (Charles River, Germany), 4 weeks old, were used. The animal studies were conducted in accordance with the recommendations of the European Community (Directive 2010/63/EU, 1st January 2013). All animal procedures were performed in strict accordance with the German regulations of the Society for Laboratory Animal Science (GV-SOLAS) and the European Health Law of the Federation of Laboratory Animal Science Associations (FELASA). Animals were excluded from further analysis if sacrifice was necessary according to the humane endpoints established by the ethical board. All experiments were approved by the ethical board of the Niedersächsisches Landesamt für Verbraucherschutz und Lebensmittelsicherheit, Oldenburg, Germany. Compounds **10** and **26** were administered at 1 mg/kg intravenously in a cassette format (n=2). At the time points 0.25, 0.5, 1, and 3 post administration, up to 25 µL of blood were collected from the lateral tail vein. At 5 h post administration, mice were euthanized to collect blood from the heart as well as to remove spleen and liver aseptically. Whole blood was collected into Eppendorf tubes coated with 0.5 M EDTA and immediately spun down at 15870 x g for 10 min at 4 °C. Then, plasma was transferred into a new Eppendorf tube spleen and liver were homogenized using a Polytron tissue homogenizer. Spleen, liver and plasma samples were stored at -80 °C until analysis. First, a calibration curve was prepared by spiking different concentrations of **10** and **26** into mouse plasma, homogenized spleen or homogenized liver from CD-1 mice. Glipizide was used as an internal standard. In addition, quality control samples (QCs) were prepared for **10** and **26** in the same matrices. For **10** and **26** the same extraction procedure was used: 7.5 µL of a plasma sample (calibration samples, QCs or PK samples) was extracted with 22.5 µL of acetonitrile containing 12.5 ng/mL of glipizide as an internal standard for 5 min at 2000 rpm on an Eppendorf MixMate® vortex mixer. Then samples were spun down at 13,000 rpm for 10 min. Supernatants were transferred to standard HPLC-glass vials. For liver and spleen, 20 µL of a sample (calibration samples, QCs or PK samples) were extracted with 10 µL water containing 10 % formic acid, and 22.5 µL acetonitrile with 12.5 ng/mL of glipizide as internal standard. Samples were extracted for 5 min at 800 rpm on an Eppendorf MixMate® vortex mixer and spun down for 5 min at 4000 rpm. Peaks of PK samples were quantified using the calibration curve. The accuracy of the calibration curve was determined using QCs independently prepared on different days (Table S1). PK parameters were determined using a non-compartmental analysis with PKSolver.<sup>22</sup>

## ASSOCIATED CONTENT

**Supporting Information.** “This material is available free of charge via the Internet at <http://pubs.acs.org>.” Further details about cell extract, affinity matrix and sample preparations for the target fishing experiments as well as data

analysis. Supplementary reaction and characterization data of all final compounds.

## AUTHOR INFORMATION

### Corresponding Author

\***Anna K. H. Hirsch** – *Helmholtz Institute for Pharmaceutical Research (HIPS), Helmholtz Centre for Infection Research (HZI), Saarland University, Campus E8.1, 66123 Saarbrücken, Germany;*  
Email: [Anna.hirsch@helmholtz-hips.de](mailto:Anna.hirsch@helmholtz-hips.de)

### Present Addresses

†If an author's address is different than the one given in the affiliation line, this information may be included here.

### Author Contributions

ψ Second authors with equal contribution. D.W., E.D., M.M.H., M.W., and A.K.H.H. coordinated the project; Synthesis and characterization of the compounds was performed by D.W., E.D., M.M.H., and M.W.; HTS and biological evaluation of derivatives against *PflspD* was performed by B.I. and M.F.; Evaluation of the potency against *PfNF54* was performed by P.B. and M.R.; Development of the LC-MS based *IspD* assay and kinetic characterization was performed by A.A. and L.B.; ADMET and PK profiling experiments were executed by A.K. and K.R.; D.W. wrote the manuscript. The manuscript was written through contributions of all authors. All authors have given approval to the final version of the manuscript.

### Funding Sources

This project has received funding from the European Union's Horizon 2020 research and innovation programme under the Marie Skłodowska-Curie grant agreement No 860816. MepAnti

### Notes

The authors declare no competing financial interest.

Figure 2, scheme 1 and the graphical abstract were created with BioRender.com

## ACKNOWLEDGMENT

D.W. Thank you Simone Amann, Jeannine Jung and Jannine Seelbach for the great work. K.R. receives funding from the German Center for Infection Research (DZIF, TTU 09.719). K.R. thanks Andrea Ahlers, Kimberley Vivien Sander, Janine Schreiber and Jennifer Wolf for excellent technical assistance.

## ABBREVIATIONS

AMR, antimicrobial resistance; AUC<sub>0-t</sub>, area under the concentration-time curve from time zero to time t; CDP-ME, 4-diphosphocytidyl-2-C-methylerythritol; CL<sub>obs</sub>, clearance (based on observed last time point with measurable concentration); CTP, cytidine triphosphate; CuAAC, copper-catalyzed azide-alkyne cycloaddition; DDA, data-dependent acquisition; DIA, data-independent acquisition; DCM, dichloromethane; DMADP, dimethylallyl diphosphate; DMF, *N,N*-dimethylformamide; DMSO, dimethyl sulfoxide; Eq, equivalents; ESI, electron spray ionization; FA, formic acid; EC<sub>50</sub>, fifty percent inhibitory concentrations; HESI, heated electrospray ionization; HTS, high throughput screening; HPLC, high pressure liquid chromatography; IDP, isopentenyl

diphosphate; IV, intravenous; Km, Michaelis constant; LCMS, liquid chromatography-mass spectrometry; MEP, 2-C-methylerythritol-D-erythritol-4-phosphate; MRT, mean residence time; MWD, multiple wave detector; n.a., no activity; ND, not detected; NMR, nuclear magnetic resonance; Pf, *Plasmodium falciparum*; PPI, inorganic diphosphate; PK, pharmacokinetic; SAR, structure-activity relationship; SD, standard deviation Vz\_obs, Volume of distribution associated with the terminal phase;

## REFERENCES

- (1) Dadgostar, P. Antimicrobial Resistance: Implications and Costs. *Infect Drug Resist.* **2019**, Volume 12, 3903-3910.
- (2) Cassini, A.; Högberg, L. D.; Plachouras, D.; Quattrocchi, A.; Hoxha, A.; Simonsen, G. S.; Colomb-Cotinat, M.; Kretzschmar, M. E.; Devleeschauwer, B.; Cecchini, M.; Ouakrim, D. A.; Oliveira, T. C.; Struelens, M. J.; Suetens, C.; Monnet, D. L. Attributable deaths and disability-adjusted life-years caused by infections with antibiotic-resistant bacteria in the EU and the European Economic Area in 2015: a population-level modelling analysis. *Lancet Infect. Dis.* **2019**, 19 (1), 56-66.
- (3) Kozlov, M. Resistance to front-line malaria drugs confirmed in Africa. *Nature* **2021**, 597, 604.
- (4) Masini, T.; Kroezen, B. S.; Hirsch, A. K. H. Druggability of the enzymes of the non-mevalonate-pathway. *Drug Discovery Today* **2013**, 18 (23), 1256-1262.
- (5) Diamanti, E.; Hamed, M. M.; Lacour, A.; Bravo, P.; Illarionov, B.; Fischer, M.; Rottmann, M.; Witschel, M.; Hirsch, A. K. H. Targeting the IspD Enzyme in the MEP Pathway: Identification of a Novel Fragment Class. *ChemMedChem* **2022**, 17, e202100
- (6) Mombo-Ngoma, G.; Remppis, J.; Sievers, M.; Zoleko Manego, R.; Endamne, L.; Kabwende, L.; Veletzky, L.; Nguyen, T. T.; Groger, M.; Lötsch, F.; Mischlinger, J.; Flohr, L.; Kim, J.; Cattaneo, C.; Hutchinson, D.; Duparc S.; Moehrl, J.; Velavan, T. P.; Lell B.; Ramharter, M.; Adegnik, A. A.; Benjamin Mord-müller, B.; Kremsner, P. G. Efficacy and Safety of Fosmidomycin-Piperaquine as Nonartemisinin-Based Combination Therapy for Uncomplicated Falciparum Malaria: A Single-Arm, Age De-escalation Proof-of-Concept Study in Gabon. *Clinical Infectious Diseases*, **2018**, 66 (12), 1823-1830.
- (7) Frank, A.; Groll, M. The Methylerythritol Phosphate Pathway to Isoprenoids. *Chemical Reviews*. **2017**, 117 (8), 5675-5703.
- (8) Price, K. E.; Armstrong, C. M.; Imlay, L. S.; Hodge, D. M.; Pidathala, C.; Roberts, N. J.; Park, J.; Mikati, M.; Sharma, R.; Lawrenson, A. S.; Tolia, N. H.; Berry, N. G.; O'Neill, P. M.; John, A.R.O. Molecular Mechanism of Action of Antimalarial Benzothiazolones: Species-Selective Inhibitors of the Plasmodium spp. MEP Pathway enzyme, IspD. *Sci Rep.* **2016**, 6, 12.
- (9) Mathew, J.; Ding, S.; Kunz, K. A.; Stacy, E. E.; Butler, J. H.; Haney, R. S.; Merino, E. F.; Butschek, G. J.; Rizopoulos, Z.; Totrov, M.; Cassera, M. B.; Carlier, P. R. Malaria Box-Inspired Discovery of N-Aminoalkyl- $\beta$ -carboline-3-carboxamides, a Novel Orally Active Class of Antimalarials. *ACS Med. Chem. Lett.* **2022**, 13 (3), 365-370.
- (10) Imlay, L. S.; Armstrong, C. M.; Masters, M. C.; Li, T.; Price, K. E.; Edwards, R. L.; Mann, K. M.; Li, L. X.; Stallings, C. L.; Berry, N. G.; O'Neill, P. M.; Odom, A. R. Plasmodium IspD (2-C-Methyl-D-erythritol 4-Phosphate Cytidyltransferase), an Essential and Druggable Antimalarial Target. *ACS Infect. Dis.* **2015**, 1 (4), 157-167.
- (11) Ding, S.; Ghavami, M.; Butler, J. H.; Merino, E. F.; Slobodnick, C.; Cassera, M. B.; Carlier, P. R. Probing the B- & C-rings of the antimalarial tetrahydro- $\beta$ -carboline MMV008138 for steric and conformational constraints. *Bioorganic Med. Chem. Lett.* **2020**, 30 (22), 127520.
- (12) Wu, W.; Herrera, Z.; Ebert, D.; Baska, K.; Cho, S. H.; Derisi, J. L.; Yeh, E. A. Chemical Rescue Screen Identifies a Plasmodium falciparum Apicoplast Inhibitor Targeting MEP Isoprenoid Precursor Biosynthesis. *Antimicrobial Agents and Chemo-therapy* **2015**, 59 (1), 356-364.
- (13) Honold, A.; Lettl, C.; Schindele, F.; Illarionov, B.; Haas, R.; Witschel, M.; Bacher, A.; Fischer, M.; Inhibitors of the Bifunctional 2-C-Methyl-D-erythritol 4-Phosphate Cytidylyl Transferase/2-C-Methyl-D-erythritol-2,4-cyclopyrophosphate Synthase (IspDF) of *Helicobacter pylori*. *Helv. Chim. Acta*, **2019**, 102, e1800228.
- (14) Ziku, L.; Sharkey, T. D.; Metabolic profiling of the methylerythritol phosphate pathway reveals the source of post-illumination isoprene burst from leaves. *Plant, Cell and Environment*, **2013**, 36, 429-437.
- (15) Konstantinović, J.; Kany, A. M.; Alhayek, A.; Abdelsamie, A.; Sikandar, A.; Voos, K.; Yao, Y.; Andreas, A.; Shafiei, R.; Loretz, B.; Schönauer, E.; Bals, R.; Brandstetter, H.; Hartmann, R. W.; Ducho, C.; Lehr, C.; Beisswenger, C.; Müller, R.; Rox, K.; Hauptenthal, J.; Hirsch, A. K. H.; Inhibitors of the Elastase LasB for the Treatment of Pseudomonas aeruginosa Lung Infections. *ACS Cent. Sci.* **2023**, 9, 12, 2205-2215
- (16) Ghavami, M.; Merino, F. E.; Yao, Z.; Elahi, R.; Simpson, M. E.; Fernández-Murga, M. L.; Butler, J. H.; Casasanta, M. A.; Krai, P. M.; Totrov, M. M.; Slade, D. J.; Carlier, P. R.; and Cassera, M. B. Biological Studies and Target Engagement of the 2-C-Methyl-d-Erythritol 4-Phosphate Cytidylyltransferase (IspD)-Targeting Antimalarial Agent (1R,3S)-MMV008138 and Analogs. *ACS Infect. Dis.* **2018**, 4, 4, 549-559
- (17) Witschel, M.C., Höffken, H.W., Seet, M., Parra, L., Mietzner, T., Thater, F., Niggeweg, R., Röhl, F., Illarionov, B., Rohdich, F., Kaiser, J., Fischer, M., Bacher, A. and Diederich, F., Inhibitors of the Herbicidal Target IspD: Allosteric Site Binding. *Angew. Chem. Int. Ed.*, **2011**, 50: 7931-7935. <https://doi.org/10.1002/anie.201102281>
- (18) Aebersol, R.; Mann, M.; Mass-spectrometric exploration of proteome structure and function, *Nature*, **2016** Sep 15;537(7620):347-55.
- (19) Kuzmic, P. Program DYNAFIT for the analysis of enzyme kinetic data: application to HIV proteinase, *Anal. Biochem.* **1996**, 237, 260-273.
- (20) Snyder, C.; Chollet, J.; Santo-Tomas, J.; Scheurer, C.; Wittlin, S. In vitro and in vivo interaction of synthetic peroxide RBX1160 (OZ277) with piperaquine in Plasmodium models, *Exp Parasitol* **2007**, 115(3), 296-300.
- (21) Huber, W., and Koella, J.C. A comparison of three methods of estimating EC50 in studies of drug resistance of malaria parasites. *Acta Trop.*, **1993**, 55(4), 257-261.
- (22) Zhang, Y.; Huo, M.; Zhou, J.; Xie, S.; PKSolver: An add-in program for pharmacokinetic and pharmacodynamic data analysis in Microsoft Excel, *Comput. Methods Programs Biomed.* **2010**, 3, 306-314.

